Anonymous Referee #3

This work did a nice job in measuring the chemical composition and mixing states of aerosols at an urban and a rural site in Beijing. More than 4 million particles were detected at each site, of which the chemically analyzed particles were grouped and analyzed to investigate the potential sources and atmospheric processing. The authors found that the urban particles were influenced significantly by rural processing and transport. The paper is generally well-written, and I recommend it for publication after some addressing the following comments.

Comments: 1. The authors listed several studies in paragraph 2 in Introduction, but didn't contain any conclusion. What does it mean by "discrepancies remain among these studies"? Authors need to be more specific about what discrepancies exist among the studies. Please revise/rephrase and be more specific.

Ans: We have added the following passage to illustrate the discrepancies and gaps in knowledge (lines 53–62):

"For example, the mass loading of $PM_{2.5}$ can rapidly increase to hundreds µg m^{-3}. Both Wang et al. (2016) and Cheng et al. (2016) suggested the secondary formation of sulfate from the

oxidation of NO_2, while Guo et al. (2014) proposed a mechanism of particle formation and growth. Different from local secondary formation and accumulation, Li et al. (2015) proposed that particles via long-range transport cause the elevation of $PM_{2.5}$. According to Sun et al. (2014) and Zhai et al. (2016), regional transport played an important role during heavy haze episodes. However, most studies have focused on the urban areas of Beijing, with limited attention paid to rural areas. To illustrate the sources, evolution, and transport of particles, the investigation of rural areas around Beijing is necessary."

2. It should be noted that chemical bias of SPAMS might introduce uncertainties in representativeness of ambient particles and even in classification of chemically analyzed particles. I think there is a need to mention this caveat in your paper, and caution the readers that uncertainties may be expected for the results. This can be provided either in Introduction or Discussions.

Ans: We completely agree with the reviewer that the limitations of the instrumentation should be addressed (lines70–72).

"Due to the nature of laser desorption/ionization (LDI), the instrument is very sensitive to dust and other types of particles containing sodium and potassium, and this may cause bias in the particle matrix (Pratt and Prather, 2012)."

3. Please clarify the differences between this study and previous studies. The significance of this study is not well written in the paper.

Ans: Associated with what we mentioned in Lines 76–83, we have added the following paragraph:

"Organics, sulfate, nitrate, ammonium and other species have been found internally mixed in the atmospheric particles, and these particle types are mostly from the combustion of fuel or biomass. The abundance of secondary species can indicate the degree of aging during atmospheric processing. Particles are more secondary species with deeper processing. However, these studies lack the use of this data to provide a view of the dynamic particulate processing. Therefore, we used the relative abundance of secondary species to adequately illustrate the process of single particles at both sites, providing a tracing system on a regional scale."

4. L150: The EC category has four types including EC-Nitrate (EC-Nit), EC-Sulfate (EC-Sul), and EC-Nit-Sul. Is it "four", not "three"? Or there is another type?

Ans: Sorry, that was is a typo. We have changed it to "three."

5. According to line 243, K-rich is one of branches of k-rich category. According to Figure 6a, K-rich means BB (BB in figure 6 caption, and K-rich in the figure) According to line 366, BB-related particle means K-rich category. The use of K-rich category, K-rich type, BB and BB-related particle is confusing. Please make the description more clear, specific and concrete.

Ans: Thank you very much for this suggestion. The K-rich category is from BB-related particles, and we will stick to this term. We have changed our description in the text, as well as the caption of Figure 6a.

6. As you mentioned in Line 253, the household BB is prohibited in urban Beijing,

which is inconsistent with figure 6c indicating that the highest number counts of K-rich were observed when wind speed was less than 2 m s-1, is that possible K-rich_PKU can also from other sources?

Ans: This is a very interesting question.

The urban sampling site is around the 4th ring expressway of Beijing, 10 km from the 5th ring expressway. In these areas, there are still villages in which biofuels are used. Therefore, these K-rich_PKU were also from biomass burning.

7. L295: "mass spectra of NaK category contained f Na+, K+ . . ." Please correct.

Ans: We have made the correction (line 319).

References

Cheng, Y., Zheng, G., Wei, C., Mu, Q., Zheng, B., Wang, Z., Gao, M., Zhang, Q., He, K., and Carmichael, G.: Reactive nitrogen chemistry in aerosol water as a source of sulfate during haze events in China, Science Advances, 2, e1601530, 2016.

Guo, S., Hu, M., Zamora, M. L., Peng, J., Shang, D., Zheng, J., Du, Z., Wu, Z., Shao, M., Zeng, L., Molina, M. J., and Zhang, R.: Elucidating severe urban haze formation in China, Proc Natl Acad Sci U S A, 111, 17373-17378, 10.1073/pnas.1419604111, 2014.

Li, P., Yan, R., Yu, S., Wang, S., Liu, W., and Bao, H.: Reinstate regional transport of PM2.5 as a major cause of severe haze in Beijing, Proc Natl Acad Sci U S A, 112, 2015.

Pratt, K. A., and Prather, K. A.: Mass spectrometry of atmospheric aerosols--recent developments and applications. Part II: On-line mass spectrometry techniques, Mass Spectrom. Rev., 31, 17-48, 10.1002/mas.20330, 2012.

Sun, Y., Jiang, Q., Wang, Z., Fu, P., Li, J., Yang, T., and Yin, Y.: Investigation of the sources and evolution processes of severe haze pollution in Beijing in January 2013, J. Geophys. Res. Atmos., 119, 4380-4398, 10.1002/2014jd021641, 2014.

Wang, G., Zhang, R., Gomez, M. E., Yang, L., Zamora, M. L., Hu, M., Lin, Y., Peng, J., Guo, S., and Meng, J.: Persistent sulfate formation from London Fog to Chinese haze, Proceedings of the National Academy of Sciences, 113, 13630-13635, 2016.

Zhai, S., An, X., Zhao, T., Sun, Z., Hou, Q., and Wang, C.: Detecting critical $PM_{2.5}$ emission sources and their contributions to a heavy haze episode in Beijing, China by using an adjoint model, Atmospheric Chemistry and Physics Discussions, 2016, 1-20, 10.5194/acp-2016-911, 2016.

The authors performed simultaneous observations of size-resolved single-particle chemical composition and mixing state in both urban and rural areas of Beijing. The campaigns collected more than 4 million particles being at both sites. The authors have investigated the different sources, processing, and origination of atmospheric particles at both sites. Generally, the manuscript illustrates a substantial contribution to the scientific understanding of urban particulate pollution in China. Particularly, the clustering strategy used in this work can be very useful to illustrate different stages of atmospheric processing. The manuscript is concisely organized and well written. Therefore, the reviewer prefers publishing if the following concerns are addressed.

Major comments

1. The statement in the Introduction should be more clarified between Lines 47–53. The discrepancies should be described, and a conclusion or hypothesis should have been drawn from the literature review.

Ans: The following passage has been added to the text (lines 53–62):

"For example, the mass loading of PM$_{2.5}$ can rapidly increase to hundreds μg m^{-3}. Both Wang et al. (2016) and Cheng et al. (2016) suggested the secondary formation of sulfate from the oxidation of NO$_2$, while (Guo et al., 2014) proposed a mechanism of particle formation and growth. Different from local secondary formation and accumulation, Li et al. (2015) proposed that particles via long-range transport cause the elevation of PM$_{2.5}$. According to Sun et al. (2014) and Zhai et al. (2016), regional transport plays an important role during heavy haze episodes. However, most studies have focused on the urban areas of Beijing, with limited attention paid to rural areas. To illustrate the sources, evolution, and transport of particles, the investigation of rural areas around Beijing is necessary."

2. Also, could you be specific on this "limited attention to the atmospheric particulate processing?" It is very important because it provides the novelty of this work compared to previous studies.

Ans: We completely agree with the reviewer. The following statement has been added to the text to enhance the argument (lines 76−83):

"Organics, sulfate, nitrate, ammonium and other species have been found internally mixed in the atmospheric particles, and these particle types are mostly from the combustion of fuel or biomass. The abundance of secondary species can indicate the degree of aging during atmospheric processing. Particles are with more secondary species with deeper processing. However, these studies lack the use of this data to provide a view of the dynamic particulate processing. Therefore, we used the relative abundance of secondary species to adequately illustrate the process of single particles

at both sites, providing a tracing system on a regional scale."

3. Lines 101–112. The use of relative peak area to determine the aging of particles is interesting. As we know, matrix effect could alter the ion intensities of each ion. The authors should address the possible influential factor for bias.

Ans: We have added this part to the text (lines 128–131):

"Indeed, the matrix effect can affect ionic intensities between different particles during single-particle mass spectrometer analysis. However, the effect can be reduced by using the average mass spectra of particles within a similar size distribution and chemical composition."

4. Table 1. The reviewer strongly suggests a column of comment on the source of particle types at both sites, respectively.

Ans: We have added a comment on the sources of particles.

5. Section 3.2.5. Is it possible to use the polar plots at both sites to locate the potential source of Fe-rich particles?

Ans: Yes, according to the polar plots at both sites, the Fe-rich particles originated from the south of both sites which is the direction of Hebei Province, as we described in the text.

6. Please compare the -Sul particles at both sites because the sulfate-rich particles can be formed from the oxidation of SO2. Any difference in the origin of sulfate-rich particles at different sites? Please add additional analysis or comments to Discussion.

Ans: A detailed interpretation of sulfate-rich particles has been added in lines 433–446:

"SO$_2$ was strictly controlled in Beijing. However, the emission of SO$_2$ is still significant

in the nearby Hebei and Shandong provinces (Shi et al. 2019). The different control measures produced a low concentration area of SO_2 around Beijing. Sulfate-rich particle types such as EC-Sul, OC-Sul, K-Sul, and NaK-Sul usually arrived at the PKU site when the wind speed was high (> 3m s^{-1}). The wind directions, along with the transport of sulfate-rich particles, were east, southwest and south. In these directions, sulfate was either primarily emitted from coal burning for residential heating, power generation and industry, or secondary uptake on pre-existing particles (Zhang et al., 2015). Likewise, a portion of sulfate-rich particle arrived at the PG site when the wind speed was high. However, locally formed sulfate was also pronounced, especially for ECOC-Sul, K-Sul, and NaK-Sul. As discussed in Section 3, ECOC-Sul and NaK-Sul were mainly from coal burning for residential heating, and K-Sul was formed due to the uptake of secondary sulfate. Conclusively, the particulate characterization in rural areas around Beijing is significantly influenced by residential coal burning."

7. Section 3.4. according to the claim in the manuscript, both OC-PG and ECOC-PG are supposed to be local. However, the polar plot suggests that these particle types are from multiple directions, please explain.

Ans: Yes, OC_PG was mainly from the east, south, and west, and ECOC_PG came from the northeast, southeast, and east. They certainly came from multiple directions. However, the highest concentrations of these particles were at the centers of the polar plots, indicating that emissions of OC_PG and ECOC_PG were high in the Beijing region. Therefore, the following statement has been added to line 381:

"Also, the emissions of OC_PG and ECOC_PG are high in the region."

Minor and technical

Lines 385: "detailed" should be "details."

Ans: We have changed this part (line 412).

Line 421. "small" should be "limited."

Ans: We have changed this part (line 421).

References

Cheng, Y., Zheng, G., Wei, C., Mu, Q., Zheng, B., Wang, Z., Gao, M., Zhang, Q., He, K., and Carmichael, G.: Reactive nitrogen chemistry in aerosol water as a source of sulfate during haze events in China, Science Advances, 2, e1601530, 2016.

Guo, S., Hu, M., Zamora, M. L., Peng, J., Shang, D., Zheng, J., Du, Z., Wu, Z., Shao, M., Zeng, L., Molina, M. J., and Zhang, R.: Elucidating severe urban haze formation in China, Proc. Natl. Acad. Sci. U.S.A., 111, 17373-17378, 10.1073/pnas.1419604111, 2014.

Li, P., Yan, R., Yu, S., Wang, S., Liu, W., and Bao, H.: Reinstate regional transport of PM2.5 as a major cause of severe haze in Beijing, Proc. Natl. Acad. Sci. U.S.A., 112, 2015.

Sun, Y., Jiang, Q., Wang, Z., Fu, P., Li, J., Yang, T., and Yin, Y.: Investigation of the sources and evolution processes of severe haze pollution in Beijing in January 2013, J. Geophys. Res. Atmos., 119, 4380-4398, 10.1002/2014jd021641, 2014.

Wang, G., Zhang, R., Gomez, M. E., Yang, L., Levy Zamora, M., Hu, M., Lin, Y., Peng, J., Guo, S., Meng, J., Li, J., Cheng, C., Hu, T., Ren, Y., Wang, Y., Gao, J., Cao, J., An, Z., Zhou, W., Li, G., Wang, J., Tian, P., Marrero-Ortiz, W., Secrest, J., Du, Z., Zheng, J., Shang, D.,

Zeng, L., Shao, M., Wang, W., Huang, Y., Wang, Y., Zhu, Y., Li, Y., Hu, J., Pan, B., Cai, L., Cheng, Y., Ji, Y., Zhang, F., Rosenfeld, D., Liss, P. S., Duce, R. A., Kolb, C. E., and Molina, M. J.: Persistent sulfate formation from London Fog to Chinese haze, Proc. Natl. Acad. Sci. U.S.A., 113, 13630-13635, 10.1073/pnas.1616540113, 2016.

Zhai, S., An, X., Zhao, T., Sun, Z., Hou, Q., and Wang, C.: Detecting critical $PM_{2.5}$ emission sources and their contributions to a heavy haze episode in Beijing, China by using an adjoint model, Atmospheric Chemistry and Physics Discussions, 2016, 1-20, 10.5194/acp-2016-911, 2016.

Zhang, R., Wang, G., Guo, S., Zamora, M. L., Ying, Q., Lin, Y., Wang, W., Hu, M., and Wang, Y.: Formation of urban fine particulate matter, Chem. Rev., 115, 3803-3855, 10.1021/acs.chemrev.5b00067, 2015.

1 Simultaneous Measurement of Urban and Rural Single Particles in Beijing, Part I:

2 Chemical Composition and Mixing State

3 Yang Chen[1], Jing Cai[2], Zhichao Wang[1], Chao Peng[1], Xiaojiang Yao[1], Mi Tian[1], Yiqun

4 Han[2], Guangming Shi[1,3], Zongbo Shi[4,5], Yue Liu[2], Xi Yang[2], Mei Zheng[2*], Tong Zhu[2],

5 Kebin He[6], Qiang Zhang[7], and Fumo Yang[3,1*]

6 [1]Center for the Atmospheric Environment Research, Chongqing Institute of Green and

7 Intelligent Technology, Chinese Academy of Sciences, Chongqing 400714, China

8 [2] SKL-ESPC and BIC-ESAT, College of Environmental Sciences and Engineering, Peking

9 University, Beijing 100871, China

10 [3]College of Architecture and Environment, Sichuan University, Chengdu 610065, China

11 [4] School of Geography Earth and Environmental Sciences, University of Birmingham,

12 Birmingham B15 2TT, UK

13 [5]Institute of Surface-Earth System Science, Tianjin University, Tianjin 300072, China

14 [6] School of Environment, Tsinghua University, Beijing 100084, China

15 [7]Department of Earth System Science, Tsinghua University, Beijing, China

16 Corresponding to Fumo Yang (fmyang@scu.edu.cn) and Mei Zheng

17 (mzheng@pku.edu.cn)

18 Keywords: urban; regional; single particle; transport; mixing state

Abstract

Two single particle aerosol mass spectrometers (SPAMS) were deployed simultaneously at an urban and a rural site in Beijing during an intensive field campaign from 1st to 29th Nov 2016 to investigate the source and process of airborne particles in Beijing. In the first part of this research, we report the single-particle chemical composition, mixing state, and evolution at both sites. 96% and 98% of collected particles were carbonaceous at the urban and rural sites, respectively. Five particle categories, including elemental carbon (EC), organic carbon (OC), internal-mixed EC and OC (ECOC), potassium-rich (K-rich), and Metals were observed at both sites. The categories were partitioned into particle types depending on different atmospheric processing stages. Seventeen particle types were shared at both sites. In the urban area, nitrate-containing particle types, such as EC-Nit and ECOC-Nit, were enriched, especially at night; sulfate-containing particles were transported when wind speed was high; ECOC-Nit-Sul were mostly local-aged. In sum, these processed particles took up to 85.3% in the urban areas. In the rural area, regional particles were abundant, but freshly emitted ECOC and OC had distinct patterns that were pronounced at cooking and heating time. Biomass burning, traffic, and coal burning were major sources of $PM_{2.5}$ in both rural and urban areas. Besides, the particles from the steel industry located in the south were also identified. In summary, the chemical composition of urban and rural particle types was similar in Beijing; the urban particles were influenced significantly by rural processing and transport. The work is useful to understand the evolution of urban and rural particles in Beijing during winter.

1. Introduction

China has experienced severe haze events caused by extremely high concentrations of fine particulate matter ($PM_{2.5}$) since January 2013. In the worst cases, an area of 2.0 million km^2 and a population of 800 million were affected (Huang et al., 2014). In the Beijing-Tianjin-Hebei (BTH) area, extreme haze events frequently occur during winter, with $PM_{2.5}$ mass reaching rapidly up to 200 µg m^{-3} and sustaining such levels for hours (Guo et al., 2014).

Over the last two decades, comprehensive studies have been conducted on urban PM in Beijing. He et al. (2001) reported the first characterization of $PM_{2.5}$. Since then, numerous studies have been published on characterization (Huang et al., 2010), sources (Guo et al., 2012; Sun et al., 2014a), and processing of PM (Sun et al., 2013). The mechanism of rapid-boosting $PM_{2.5}$ in Beijing, including new particle formation and growth (Guo et al., 2014), regional transport (Li et al., 2015), and both (Du et al., 2017; Sun et al., 2014a), have been proposed. However, discrepancies remain among these studies. For example, the mass loading of $PM_{2.5}$ can rapidly increase to hundreds µg m^{-3}. Both Wang et al. (2016) and Cheng et al. (2016) suggested the secondary formation of sulfate from the oxidation of NO_2, while (Guo et al., 2014) proposed a mechanism of particle formation and growth. Different from local secondary formation and accumulation, Li et al. (2015) proposed that particles via long-range transport cause the elevation of $PM_{2.5}$. According to Sun et al. (2014b) and Zhai et al. (2016), regional transport plays an important role during heavy haze episodes. However, most studies have focused on the urban areas of Beijing, with limited

61   attention paid to rural areas. To illustrate the sources, evolution, and transport of particles,

62   the investigation of rural areas around Beijing is necessary.

63   Single particle mass spectrometers (SPMS) have been used to investigate the size-resolved

64   chemical composition and mixing state of atmospheric particles (Gard et al., 1997; Pratt

65   and Prather, 2012). More recently, single particle aerosol mass spectrometers (SPAMS)

66   have been used in Chinese megacities such as Beijing (Li et al., 2014), Shanghai (Tao et

67   al., 2011), Guangzhou (Bi et al., 2011), Xi'an (Chen et al., 2016; Chen et al., 2019a),

68   Nanjing (Wang et al., 2015), and Chongqing (Chen et al., 2017). SPAMS has been proven

69   a useful tool for characterizing the single-particle chemical composition, mixing state, and

70   processing of atmospheric particles. Due to the nature of laser desorption/ionization (LDI),

71   the instrument is very sensitive to dust and other types of particles containing sodium and

72   potassium, and this may cause bias in the particle matrix (Pratt and Prather, 2012).

73   In Beijing, particle types, such as carbonaceous, metal, dust, K-rich, and others during

74   spring and fall, were reported (Liu et al., 2016b; Li et al., 2014). Besides, lead-containing

75   particles have also been investigated in recent studies (Ma et al., 2016; Cai et al., 2017).

76   Organics, sulfate, nitrate, ammonium and other species have been found internally mixed

77   in the atmospheric particles, and these particle types are mostly from the combustion of

78   fuel or biomass. The abundance of secondary species can indicate the degree of aging

79   during atmospheric processing. Particles are with more secondary species with deeper

80   processing. However, these studies lack the use of this data to provide a view of the

81   dynamic particulate processing. Therefore, we used the relative abundance of secondary

82   species to adequately illustrate the process of single particles at both sites, providing a

83   tracing system on a regional scale.

84   This study is a part of the APHH-Beijing (Atmospheric Pollution and Human Health in a

85   Chinese Megacity of Beijing) intensive field campaign during winter 2016 (Shi et al., 2019).

86   Two SPAMSs were deployed simultaneously at Peking University (PKU) and Pinggu (PG)

87   in order to observe both urban and rural particles in the Beijing region. The aims of the

88   study are 1) to characterize the single-particle chemical composition and mixing state; 2)

89   to investigate particulate evolution at both sites during haze events. These two objectives

90   are presented in two parts. In Part I, particle types and their atmospheric processing (e.g.,

91   origination, source, and diurnal profiles) at both sites are reported; in Part II, the detailed

92   analysis of haze events, effects of heating activities, and evidence of regional transport are

93   addressed.

94   **2. Methodology**

95   **2.1 Sampling sites**

96   The campaigns were performed simultaneously at PKU (116.32ºE, 39.99ºN) and PG

97   (117.05ºE, 40.17ºN) from 11/01/2016 to 11/29/2016. A Description of the PKU site is

98   available in the literature (Huang et al., 2006). Briefly, the site is located on the rooftop (15

99   m above the ground) on the PKU campus which is surrounded by residential and

100   commercial blocks. Trace gases (Thermo Inc. series), meteorological parameters (Vaisala

101   Inc.), and $PM_{2.5}$ (TEOM 1430) were recorded during the observation.

102   The PG site (117.053ºE, 40.173ºN) is 3 km from the PG center. The site is located in the

103   northeast of the PKU site with a distance of 70 km. The PG site also acts as a host of the

104   AIRLESS (Effects of AIR pollution on the cardiopulmonary disease in urban and peri-

105 urban residents in Beijing) Project. The meteorological data is acquired from the local

106 meteorological office. The PG village is surrounded by orchards and farmland with no

107 main road nearby on a scale of 3 km. Coal and biomass are used for domestic heating and

108 cooking in the nearby villages.

109 **2.2 Instrumentation and data analysis**

110 Two SPAMSs (Model 0515, Hexin Inc., Guangzhou, China) were deployed at both PKU

111 and PG. A technical description of SPAMS is available in (Li et al., 2011). Briefly, a

112 SPAMS has three functional parts: sampling, sizing, and mass spectrometry. In the

113 sampling part, particles within a 0.1–2.0 µm size range pass efficiently through an

114 aerodynamic lens. In the sizing unit, the aerodynamic diameter (D_{va}) is calculated using

115 the time-of-flight of particles. The particles are then decomposed and ionized into ions one-

116 by-one using a 266 nm laser. A bipolar time-of-flight mass spectrometer measures the ions

117 and generates the positive and negative mass spectra of each particle. The two instruments

118 were maintained and calibrated following the standard procedures before sampling (Chen

119 et al., 2017).

120 A neural network algorithm based on adaptive resonance theory (ART-2a) was used to

121 resolve particle types from both datasets (Song et al., 1999). The parameters used were: a

122 vigilance factor of 0.70, a learning rate of 0.05, and 20 iterations. This procedure generated

123 771 and 792 particle groups. Then, the groups were combined into particle types based on

124 similar mass spectra, temporal trends, and size distributions (Dall'osto and Harrison, 2006).

125 During combining, relative areas of nitrate and sulfate were used to distinguish the stages

126 of processing, assuming that more sulfate and nitrate can be measured if a particle is more

127   processed during its lifetime. Thus, particles with relative peak areas of sulfate and nitrate

128   larger than 0.1 were marked with nitrate (-Nit), sulfate (-Sul), respectively, or both. Indeed,

129   matrix effect can affect ionic intensities between different particles during single-particle

130   mass spectrometer analysis. However, the effect can be reduced using average mass spectra

131   of particles within the similar size distribution and chemical composition. Finally, the

132   strategy resulted in 20 and 19 particle types at PKU and PG respectively. Among them, 17

133   types appeared at both sites, and each type has identical mass spectra ($R^2 > 0.80$) between

134   each other.

135   **3. Results**

136   A total of 4,499,606 and 4,063,522 particles were collected at PKU and PG sites,

137   respectively. The size distributions peaked at 0.48 µm and 0.52 µm (Figure 1). The smaller

138   size distribution was due to a more substantial fraction of freshly-emitted particles at PG,

139   as described in Table 1. Seventeen particle types ($R^2 > 0.80$, mass spectra) were observed

140   both at PKU and PG (Table 1). These particle types were labeled with the suffixes "_PKU"

141   or "_PG" to indicate their locations. The term "particle category" stands for a group of

142   particle types with variable stages of processing.
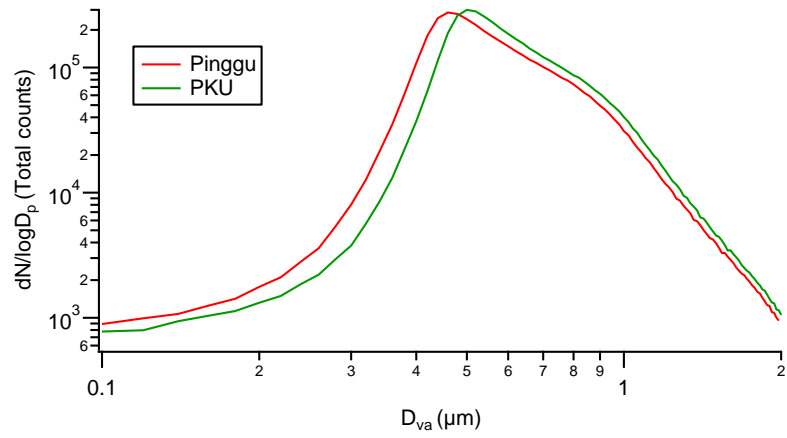
143

144   Figure 1. The size distribution of SPAMS particles at PKU and PG sites.

145

146 Table 1. SPAMS particle types identified at PKU and PG sites.

|	PKU	PKU	PG	PG	Comments
Particle type	Number	Percentage	Number	Percentage	
EC-Nit	313574	7.0	79082	2.0	Solid fuel burning, traffic
EC-Nit-Sul	473908	10.5	140107	3.5	
EC-Sul	30365	0.7	4096	0.1	
ECOC-Nit-Sul	539533	12.0	755279	18.6	Traffic, coal burning
ECOC-Sul	572548	12.7	397367	9.8	
K-rich	322731	7.2	259287	6.4	Aged biomass burning
K-Nit	359281	8.0	334547	8.2	
K-Nit-Sul	717280	16.0	76954	1.9	
K-Sul	26301	0.6	183571	4.5	
NaK	16680	0.4	74943	1.8	Coal, peat
NaK-Nit	289259	6.4	69760	1.7	
NaK-Nit-Sul	114387	2.5	77555	1.9	
NaK-Sul	7509	0.2	16578	0.4	
OC-Nit-Sul	334870	7.4	865821	21.3	Traffic,
OC-Sul	40800	0.9	279322	6.9	coal burning
Ca-dust	19869	0.4	3035	0.1	dust
Fe-rich	137600	3.1	70920	1.8	Steel industry
ECOC-Nit	137470	3.1%			Solid fuel burning
OC-Nit	41159	0.9%			Traffic, coal burning
K-Amine-Nit-Sul	4482	0.1%			Coal burning
ECOC			239953	5.9%	Coal burning
OC			135345	3.3%	Traffic, coal burning

147

148 Note: Nit stands for nitrate, Sul for sulfate.

149 **3.1 Meteorological conditions and overview**

150 Temperature, relative humidity (RH), and wind speed at both sites during the sampling

151 period are summarized in Table 2. Their temporal trends are available in Part II. The

152   average temperature at PKU (urban, 5.7±2.3 °C) was higher than at PG (rural, 3.1±2.2 °C).

153   Correspondingly, relative humidity was higher at PG (67±32%) than at PKU (49±30%).

154   The wind was stronger at PKU (2.5± 1.8 ms^{-1}) than at PG (1.7± 0.9 ms^{-1}). As shown in

155   Figure 2, at PKU, wind speed peaked at noon (local time, UTC+8), while at PG, wind speed

156   reached its maxima at 15:00. Various wind speeds determined the different dispersion

157   patterns of pollutants near the surface. It should be noticed that wind speed up to 2 ms^{-1}

158   representing a scale of 172 km in diurnal transport. Therefore, at PKU, the wind could

159   bring the pollutants from Hebei province under stagnant air conditions.

160
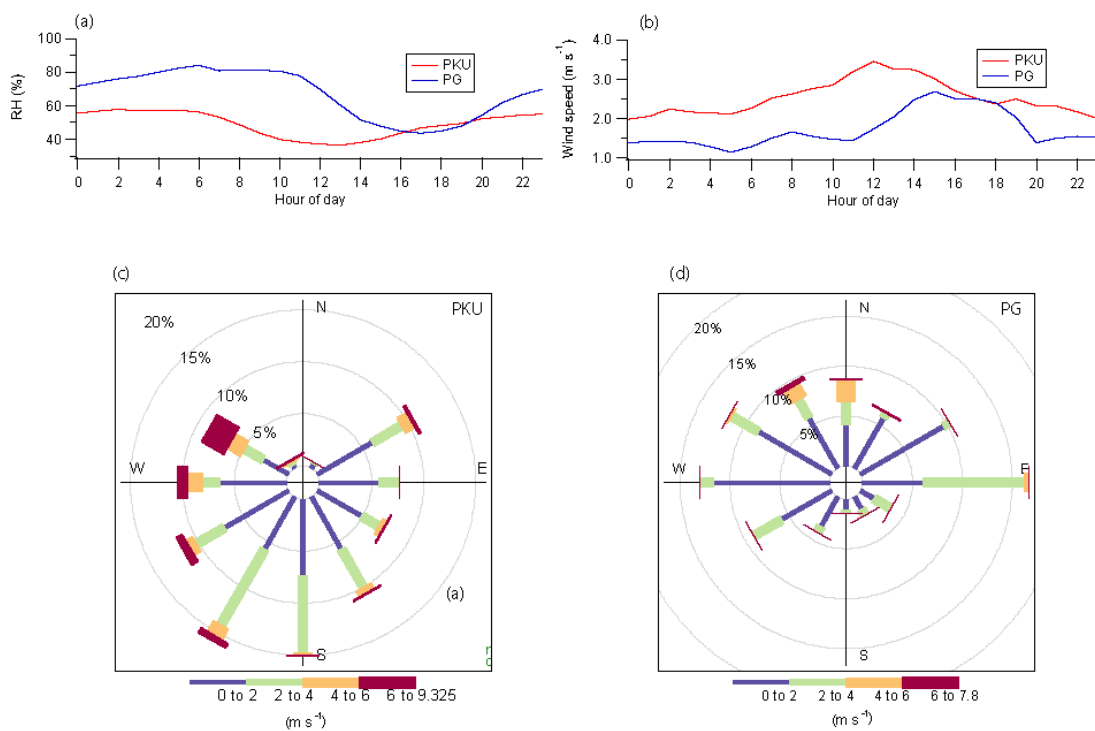
161

162   Figure 2. Diurnal plots of (a) RH and (b) wind speed, and rose plots of wind at (c)PKU and

163   (d) PG.

164

165   Table 2. Meteorological parameters at PKU and PG during the campaign.

	PKU	PG
Temperature (°C)	5.7±2.3	3.1±2.2
RH (%)	49±30	67±32
Wind speed (ms^{-1})	2.5± 1.8	1.7± 0.9

166

3.2 Common particle categories at both PKU and PG

3.2.1 Elemental carbon (EC)

169   As shown in Figure 3a, the elemental carbon (EC) particle category was represented by

170   ions peaking at m/z 12, 24, 36, 48, and 60 in positive mass spectra (Sodeman et al., 2005;

171   Toner et al., 2008). EC is emitted from solid fuel combustion, traffic (Sodeman et al., 2005;

172   Toner et al., 2008), and industrial activities (Healy et al., 2012; Liu et al., 2019a). Due to

173   the various ionic intensities of nitrate (m/z -46 and -62) and sulfate (m/z -80 and -97), the

174   EC category has four types including EC-Nitrate (EC-Nit), EC-Sulfate (EC-Sul), and EC-

175   Nit-Sul. Besides, the EC category was more abundant after the heating began rather than

176   before (Part II), indicating that coal burning was one of the primary sources.

177   EC-Nit_PKU and EC-Nit_PG accounted for 7.0% and 2.0% in PKU and PG datasets,

178   respectively. In the diurnal profiles of EC-Nit_PKU, there was an apparent early morning

179   peak at 5:00 (UTC+8, local time), along with an evening peak (22:00). There was also an

180   early morning NO$_x$ peak in the urban area of Beijing, providing sufficient precursors for

181   secondary nitrate (Shi et al., 2019). Wang et al. (2018) validated the role of N$_2$O$_5$ uptake

182   on the nitrate formation in PM. Therefore, the early morning peak of EC-Nit_PKU

183   occurred due to the uptake of nitrate on the freshly emitted EC in the early morning (Sun

184   et al., 2014a). The evening peak could be due to the low temperature after the heating

185   supply started (Liu et al., 2019a). Diurnally, EC-Nit_PG exhibited an early morning peak

186   (5:00) but no evening peak and mainly came from the southeast.

187   EC-Nit-Sul was more abundant at the rural site (18.6%) than the urban site (11.6%). EC-

188   Nit-Sul_PKU (10.5%) had early morning (04:00), morning (7:00), and afternoon peaks

189   (around 16:00), while EC-Nit-Sul_PG (3.5%) had early morning (04:00), noon, and

190   afternoon peaks (17:00, Figure 3a). However, they showed relatively small diurnal

191   variations. For example, EC-Nit-Sul_PKU varied between 800 h^{-1} and 1,000 count h^{-1}, and

192   EC-Nit-Sul_PG shifted between 200 count h^{-1} and 250 count h^{-1}. Thus, the EC-Nit-Sul at

193   both sites was most likely acting as background and regional particles (Dall'Osto et al.,

194   2016). Additionally, EC-Nit-Sul_PKU mainly came from the surrounding area in the city

195   pollutant plume, while EC-Nit-Sul_PG mainly came from the southeast (Figure 3c).

196   EC-Sul was a minor type at both sites, accounting for 0.7% at PKU and 0.1% at PG. EC-

197   Sul was pronounced in the afternoon when the wind was strong at both sites. It was unlikely

198   for either EC-Sul_PKU or EC-Sul_PG to be local because their concentrations were

199   associated with high wind speed, as shown in Figure 3c. More specifically, EC-Sul_PKU

200   came from the southeast and northeast of Hebei Province when the wind speed exceeded

201   6 m s^{-1}. EC-Sul_PG could come from the west when the wind speed exceeded 2 m s^{-1} and

202   the east when the wind speed exceeded 3 m s^{-1}, as coal-using industries are located in both

203   directions. Also, at both sites, the concentrations of SO_2 were elevated in the afternoon due

204   to transport, providing sufficient precursors for the formation of sulfate (Shi et al., 2019).
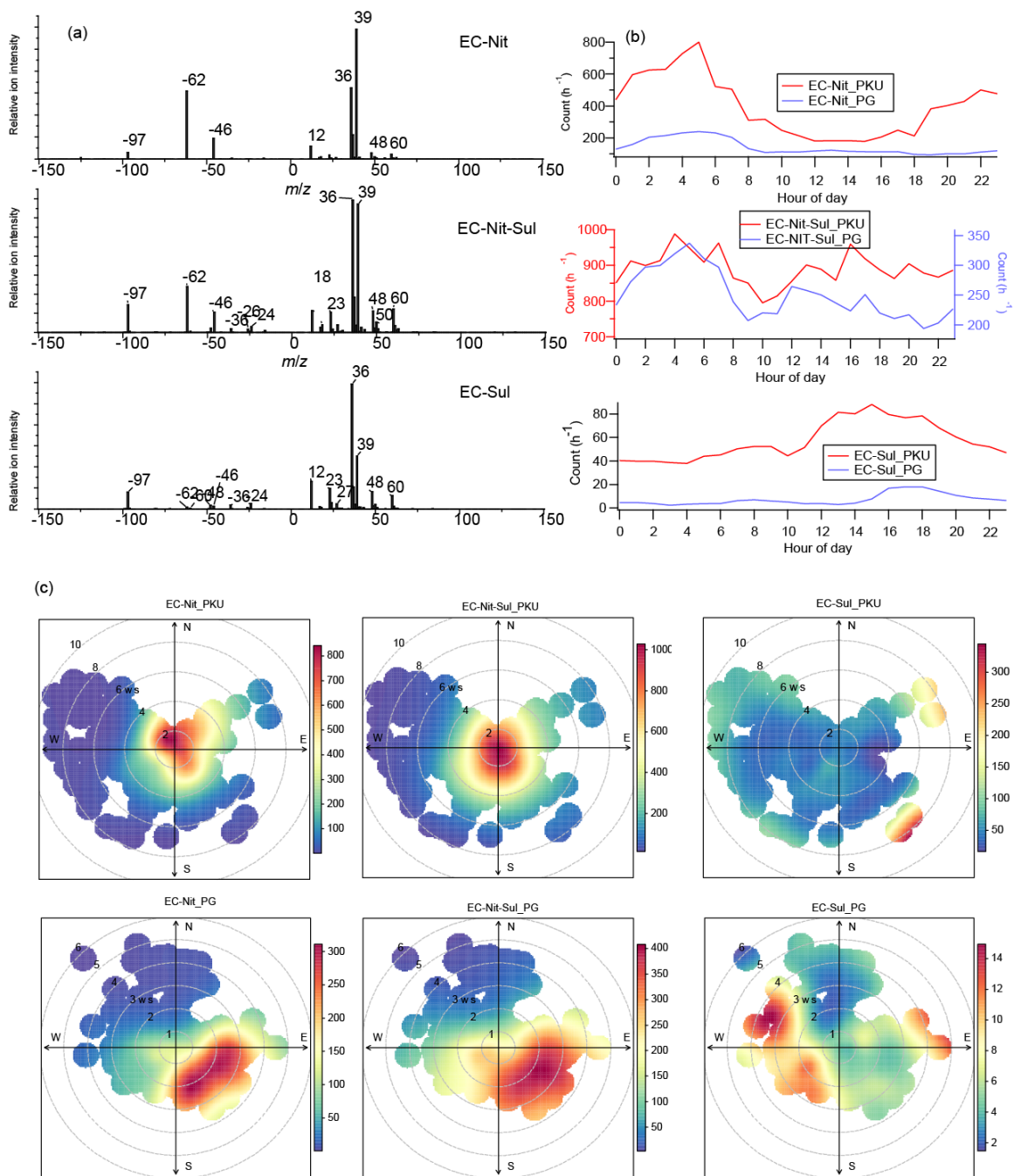
Figure 3. (a) average mass spectra of EC-Nit, EC-Nit-Sul, and EC-Sul at both sites; (b) diurnal patterns of EC-Nit, EC-Nit-Sul, and EC-Sul at both sites; (c) polar plots of EC-Nit, EC-Nit-Sul, and EC-Sul; the grey circles indicate wind speed (m s^{-1}).

3.2.2 Organic carbon (OC) category

The positive mass spectra of both OC-Nit and OC-Nit-Sul contained complicated organic ions such as $C_2H_3^+$ (*m/z* 27), C_3H^+ (*m/z* 37), $C_3H_7^+/C_2H_3O^+/$ $CHNO^+$ (*m/z* 43), $C_4H_2^+$ (*m/z* 50), aromatic hydrocarbons ($C_4H_3^+$, $C_5H_3^+$, and $C_6H_5^+$), and diethylamine ((C_2H_5)$_2NH_2^+$, *m/z* 74), (C_2H_5)$_2NCH_2^+$ (*m/z* 86)). The negative mass spectra contained CN^- (*m/z* –26), Cl^- (*m/z* –35 and 37), CNO^- (*m/z* –42), nitrate (*m/z* –46 and –62), and sulfate(*m/z* –97). The presence of CN^- and CNO^- suggests the existence of organonitrogen species (Day et al., 2010). Peak intensities of organic fragments are relatively high in the OC-Sul particles, indicating that it was relatively fresh, while OC-Nit-Sul was more processed (Zhai et al., 2015; Peng et al., 2020a). The positive mass spectrum had similar ions of Coal Combustion OA (CCOA) with significant signals of PAHs in AMS studies (Sun et al., 2013). OC-Sul showed different spatial distributions with 0.9% at PKU and 6.9% at PG.

OC-Sul_PG had morning (8:00) and afternoon (16:00) peaks, while the diurnal profile of OC-Sul_PKU showed a trend with an early morning (3:00), morning (10:00), and afternoon peaks (16:00). The diurnal trends OC-Sul at both PKU and PG were consistent with the heating pattern depending on the variation of local temperature. Moreover, OC-Sul_PG increased after the heating supply began. Polar plots suggest that OC-Sul_PKU came from surrounding southwest areas via transport, while OC-Sul_PG came from villages to the east and west (Figure 4). These results suggest that OC-Sul_PG was emitted from coal burning for residential heating in nearby areas.

OC-Nit-Sul accounted for 7.4 % and 21.3 % of all detected particles at PKU and PG, respectively. OC-Nit-Sul_PKU had a diurnal peak at 7:00 in rush hours, suggesting that

231   OC-Nit-Sul could be formed due to the uptake of nitrate on OC-Sul. While OC-Nit-Sul_PG

232   had a diurnal peak at 8:00 due to traffic in nearby towns. As an aged particle type, OC-Nit-

233   Sul_PKU and OC-Nit-Sul_PG, also acting as a similar type of background types with

234   hourly counts remained low but elevated to high levels at night. Polar plots suggest that

235   OC-Nit-Sul_PKU mainly came from the surrounding areas, while OC-Nit-Sul_PG mainly

236   came from the south and east, where populous villages are located (Figure 4).
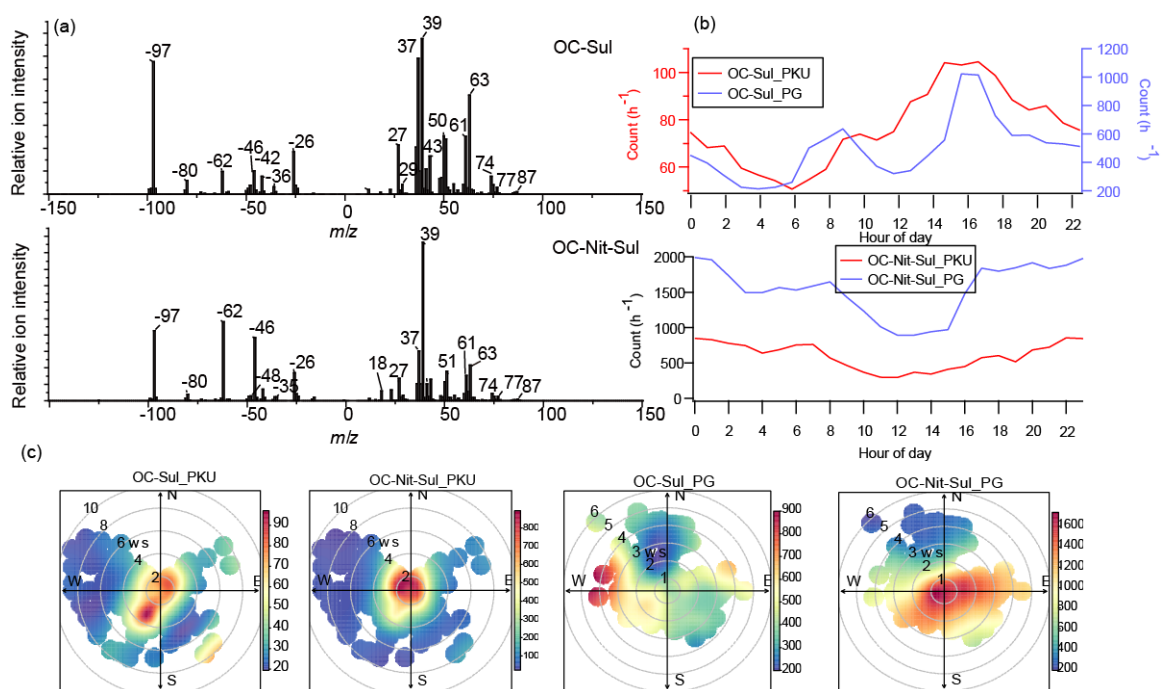
238   Figure 4. (a): average mass spectra of OC-Nit and OC-Nit-Sul observed at both sites; (b):

239   diurnal patterns of the hourly count of OC-Nit and OC-Nit-Sul at both sites; (c): polar plots

240   of OC-Sul and OC-Nit-Sul; the grey circles indicate wind speed (m s^{-1}).

241   **3.2.3 ECOC category**

242   As shown in Figure 5a, the ECOC category contained two major particle types: ECOC-

243   Nit-Sul and ECOC-Sul. The positive mass spectrum of ECOC-Nit-Sul contained C_n^+ (*m/z*

15

244   12, 24, 36…), NH_4^+ (*m/z* 18), $C_2H_3^+$ (*m/z* 27), K^+ (*m/z* 39 and 41), $C_3H_7^+$/$C_2H_3O^+$/ $CHNO^+$

245   (*m/z* 43), $C_4H_2^+$ (*m/z* 50), and $[(C_2H_5)_2NH_2]^+$ (*m/z* 74); in the negative mass spectrum, ions

246   such as sulfate (*m/z* -80 and -97), nitrate (*m/z* -46 and -62), C_n^-, and CN^- (*m/z* -26) were

247   abundant. This mixture of EC and OC particle types was common in single particle studies.

248   ECOC could be local, and from incomplete combustion processes (Chen et al., 2017), or

249   regional transport, e.g., after aging (McGuire et al., 2011; Huang et al., 2013; Zhao et al.,

250   2019). The diurnal profile of ECOC-Sul_PG showed early morning (1:00), morning (8:00),

251   and afternoon (17:00) peaks, which is consistent with local cooking and heating patterns.

252   Also, heating activities enhanced the fraction of ECOC-Sul_PG. ECOC-Sul_PKU did not

253   show a clear diurnal profile, suggesting that ECOC-Sul_PKU was mainly a background

254   type. Similarly, ECOC-Nit-Sul_PKU and ECOC-Nit-Sul_PG were also background types

255   with less obvious diurnal variations (Dall'Osto et al., 2016). Polar plots (Figure 5c)

256   suggested that both ECOC-Nit-Sul_PKU and ECOC-Sul_PKU had both local and regional

257   sources. Wind speed up to 4 m s^{-1} could cause a transport with a distance of 346 km

258   diurnally, indicating that it was possible for the particles from Hebei province to arrive at

259   the sampling place.
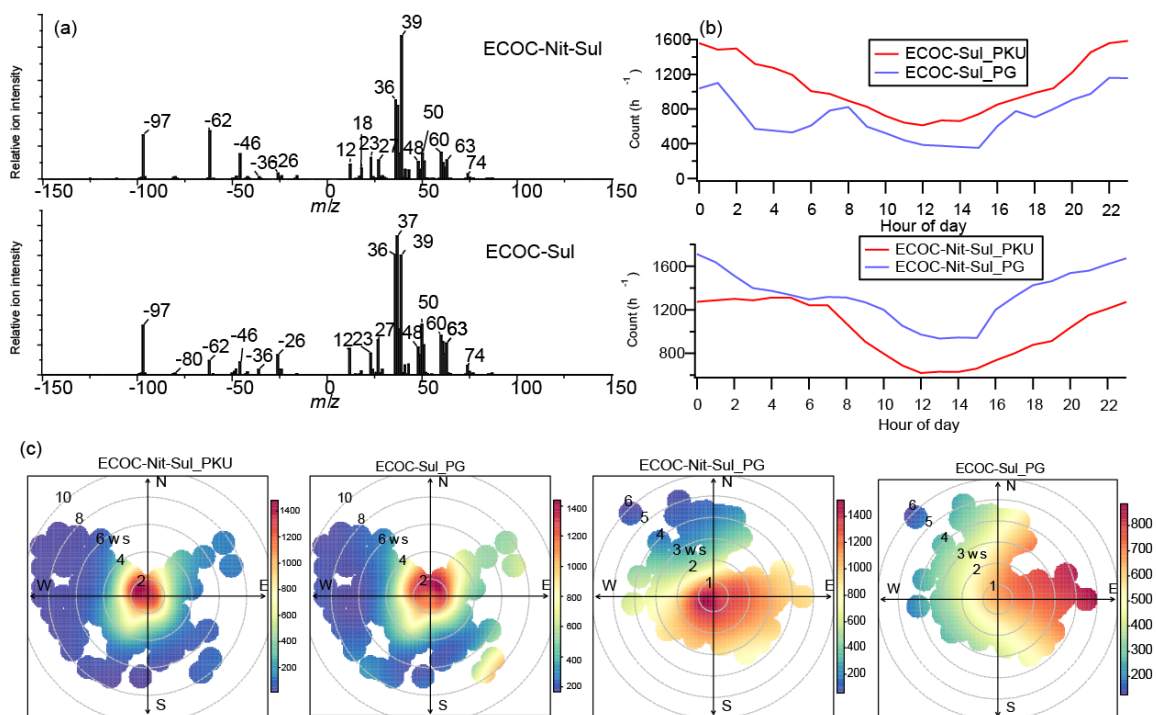
Figure 5. (a): average mass spectra of ECOC-Nit and ECOC-Nit-Sul observed at both sites; (b): diurnal patterns of the hourly count of ECOC-Sul and ECOC-Nit-Sul at both sites; (c): polar plots of ECOC-Sul and ECOC-Nit-Sul; the grey circles indicate wind speed (ms^{-1}).

3.2.4 K-rich category

Figure 6 shows a series of potassium-rich (K) particle types. K-rich contained Na$^+$ (*m/z* 23), C$_2$H$_3^+$ (*m/z* 27), C$_n^+$, C$_3$H$^+$ (*m/z* 37), K$^+$, aromatic hydrocarbons (C$_4$H$_3^+$, C$_5$H$_3^+$, and C$_6$H$_5^+$), levoglucosan (*m/z* -45, -59, and -71), sulfate, and nitrate. According to the ionic intensities of sulfate and nitrate, the K-rich particle category had several branches such as K-rich, K-Nit, K-Sul, and K-Nit-Sul. K-rich particles are commonly found in biomass burning emissions (Silva et al., 1999; Pagels et al., 2013; Chen et al., 2017). Cl$^-$ was unabundant in all K-rich particle types, suggesting that the K-rich particles had undergone aging during

17

272 atmospheric processing (Sullivan et al., 2007; Chen et al., 2016), but K-Nit, K-Nit-Sul, and

273 K-Sul were more processed.

274 All K-rich category particles showed different atmospheric evolution process at both PKU

275 and PG. K-rich_PKU illustrated a typical pattern that was at low levels in the daytime but

276 high levels at nighttime (22:00). As shown in Figure 6c, at an average wind speed of 3 m

277 s^{-1}, it took five hours for particles from a distance of 50 km to arrive at PKU. This is also

278 the reason why BB-related particles were abundant in urban Beijing where the household

279 BB is prohibited. The origination of K-rich_PKU was from nearby and southwest. K-

280 rich_PG, however, showed a pattern with cooking and heating activities, peaking at 7:00

281 and 17:00. The peak at 7:00 was due to the local emissions; the 17:00 could be transported

282 from a distance of 50 km at a wind speed of 3 m s^{-1} from the east and west.

283 The secondary process contributed to the early morning peak (5:00) of K-Nit_PKU due to

284 the nighttime formation of nitrate via hydrolysis of N_2O_5 in the NO_x-rich urban areas (Wang

285 et al., 2017). In the day time, after the rush hours, the number concentration of K-Nit_PKU

286 increased again via the uptake of nitrate due to day time photoactivity. K-Nit_PKU mainly

287 originated from the local and southerly areas (Figure 6c). Besides the early morning peak,

288 K-Nit_PG showed cooking and heating patterns that they were abundant when the

289 temperature was low in the early morning and afternoon. K-Nit_PG had wide originated

290 from both local and region via long-range transport.
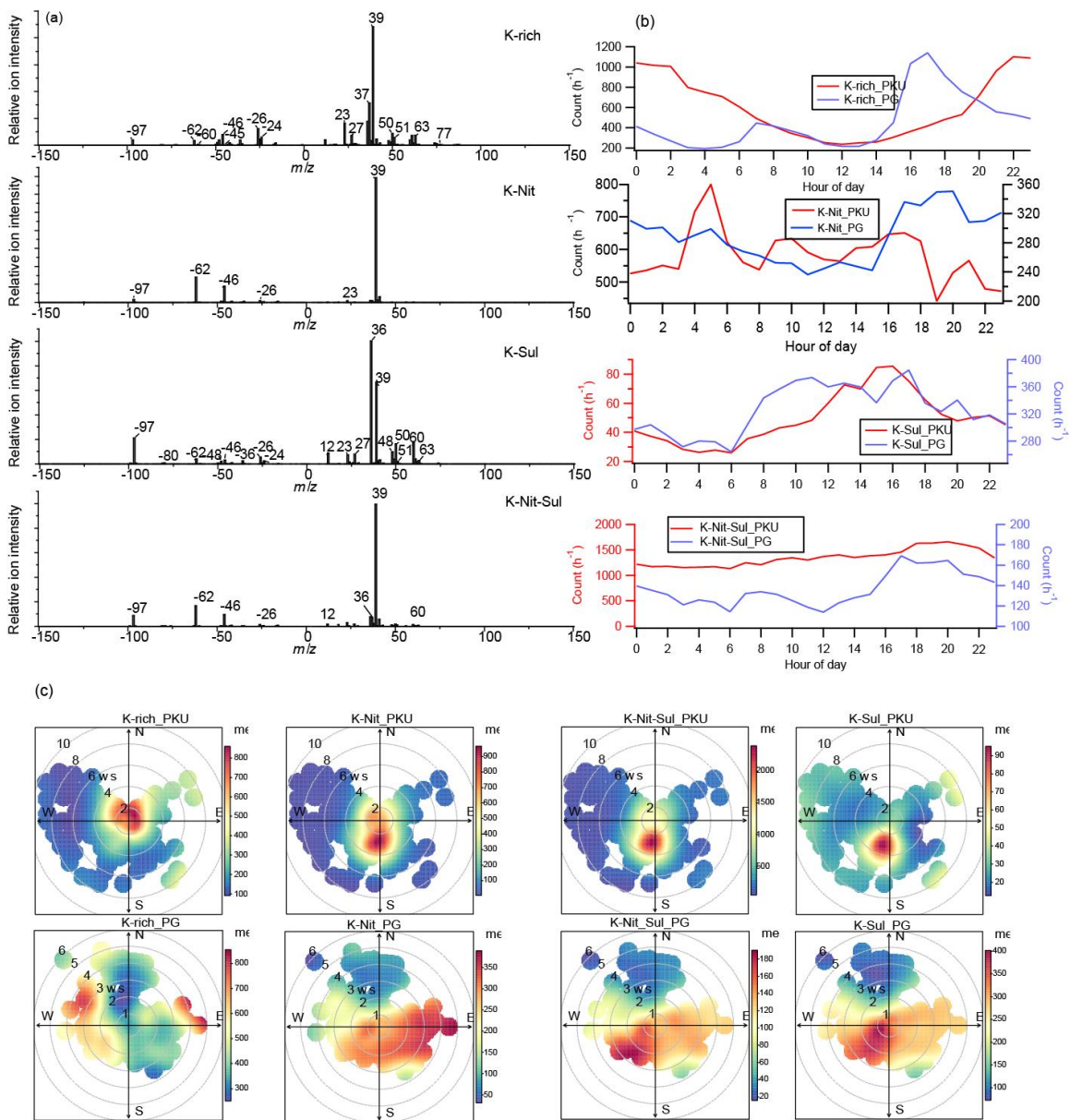
Figure 6. (a): average mass spectra of BB, K-Nit, K-Sul, and K-Nit-Sul observed at both sites; (b): diurnal patterns of the hourly count of K-rich, K-Nit, K-Sul, and K-Nit-Sul at both sites; (c): polar plots of BB, K-Nit, K-Sul, and K-Nit-Sul; the grey circles indicate wind speed (m s^{-1}).

3.2.5 Metal category

Two metal-rich particles types were identified, namely Fe-rich and Ca-rich. Fe-rich contained iron (m/z 56 and 54), K^+, Na^+, NH_4^+, Cl^- (m/z -35 and -37), sulfate, and nitrate. Ca-rich was composed of Ca^+ (m/z 40), CaO (m/z 56), K^-, Na^+, Cl^-, sulfate, and nitrate. As shown in Figure 6b, Ca-rich_PKU (0.4%) and Ca-rich_PG (0.1%) were likely of regional origin with no distinct diurnal variations. Since SiO_2^- or SiO_3^- (m/z -60 and -76) were not abundant in the Ca-rich particles, they are not likely to come from dust (Silva et al., 2000). According to its weak peaks during the rush hour at PKU, a possible source of the Ca-rich particles was from road dust re-suspension. Such rush hour peaks were not observed at PG.

Fe-rich_PKU (3.1%) and Fe-rich_PG (1.8%) had similar diurnal profiles that arose in the early morning when heavy-duty vehicles were allowed to enter the 5-ring expressway. The peak occurred earlier at PG (4:00) than (5:00) because these vehicles got close to PG earlier than to PKU. The daytime peak occurred in the afternoon at both PKU and PG when wind speed was high. Therefore, there were also multiple sources for Fe-rich particles, including re-suspended dust particles from traffic and fly ash from the steel industry. In Beijing, daytime Fe-rich particles were reported and assigned to long-range transport and industrial sources from Heibei Province (Figure 7c) (Li et al., 2014). The steel industry moved out of Beijing more than a decade ago (Liu et al., 2016b). Currently, most of these steel industries were located in the Heibei Province.
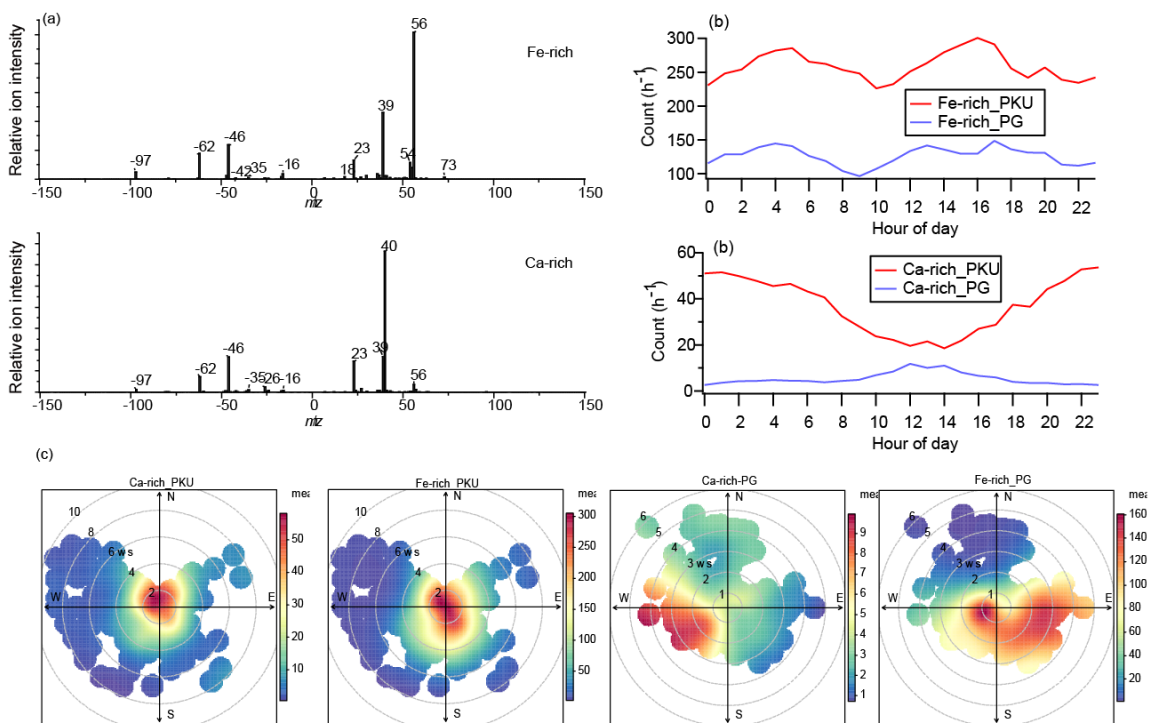
Figure 7. (a): average mass spectra of Fe-rich and Ca-rich observed at both sites; (b): diurnal patterns of the hourly count of Fe-rich and Ca-rich at both sites; (c): polar plots of Fe-rich and Ca-rich; the grey circles indicate wind speed (ms^{-1}).

3.2.6 NaK category

As shown in Figure 8, mass spectra of NaK category contained Na^+, K^+, C_n^+, C_n^-, nitrate, and PO_3^- (m/z -79). The aged NaK particles contained strong signals of nitrate (NaK-Nit), sulfate (NaK-Sul), or both (NaK-Nit-Sul). In general, the NaK category contained stronger signals of Na^+ than the EC and K-rich categories. The NaK category may also come from incomplete solid fuel combustion processes such as coal, peat, or wood (Chen et al., 2017; Healy et al., 2010; Xu et al., 2017). NaK category was more abundant at PKU (9.5%) than PG (5.8%), suggesting a stronger contribution of emission from coal boilers (Xu et al.,

21

327 2017; Xu et al., 2018). Additionally, after heating began, the fraction of NaK-Nit_PG and

328 NaK-Sul-Nit_PG increased by 1.2 times (see Part II).

329 NaK_PKU showed no distinct diurnal variations, suggesting that it was a regional particle

330 type arriving at the PKU site via transport, while NaK_PG showed an apparent diurnal

331 variation consistent with cooking and heating pattern. Polar plots also suggest that they are

332 from the east and the west. NaK-Nit, with a considerable uptake of nitrate, was more

333 abundant at PKU (6.4%) than PG (1.7%). Both NaK-Nit_PKU and NaK-Nit _PG increased

334 in the afternoon when photochemical activities were most active (Figure 8c). Both of them

335 may be from regional transport (Figures 8b and 8c).

336 NaK-Sul was a minor particle type at both PG and PKU, accounting for 0.2% and 0.4%,

337 respectively. The diurnal profile of NaK-Sul_PG was also following the local cooking and

338 heating pattern, while NaK-Sul_PKU showed a typical transport pattern that became

339 abundant in the afternoon as the southwestern wind speed increased. As a heavily aged

340 particle type, NaK-Nit-Sul was transported to both PKU and PG from the southwest. In

341 short, NaK-related particle types mainly came from the solid fuel burning process, e.g.,

342 coal. Due to its different origins, it showed different levels of processing at PKU and PG,

343 respectively.

344
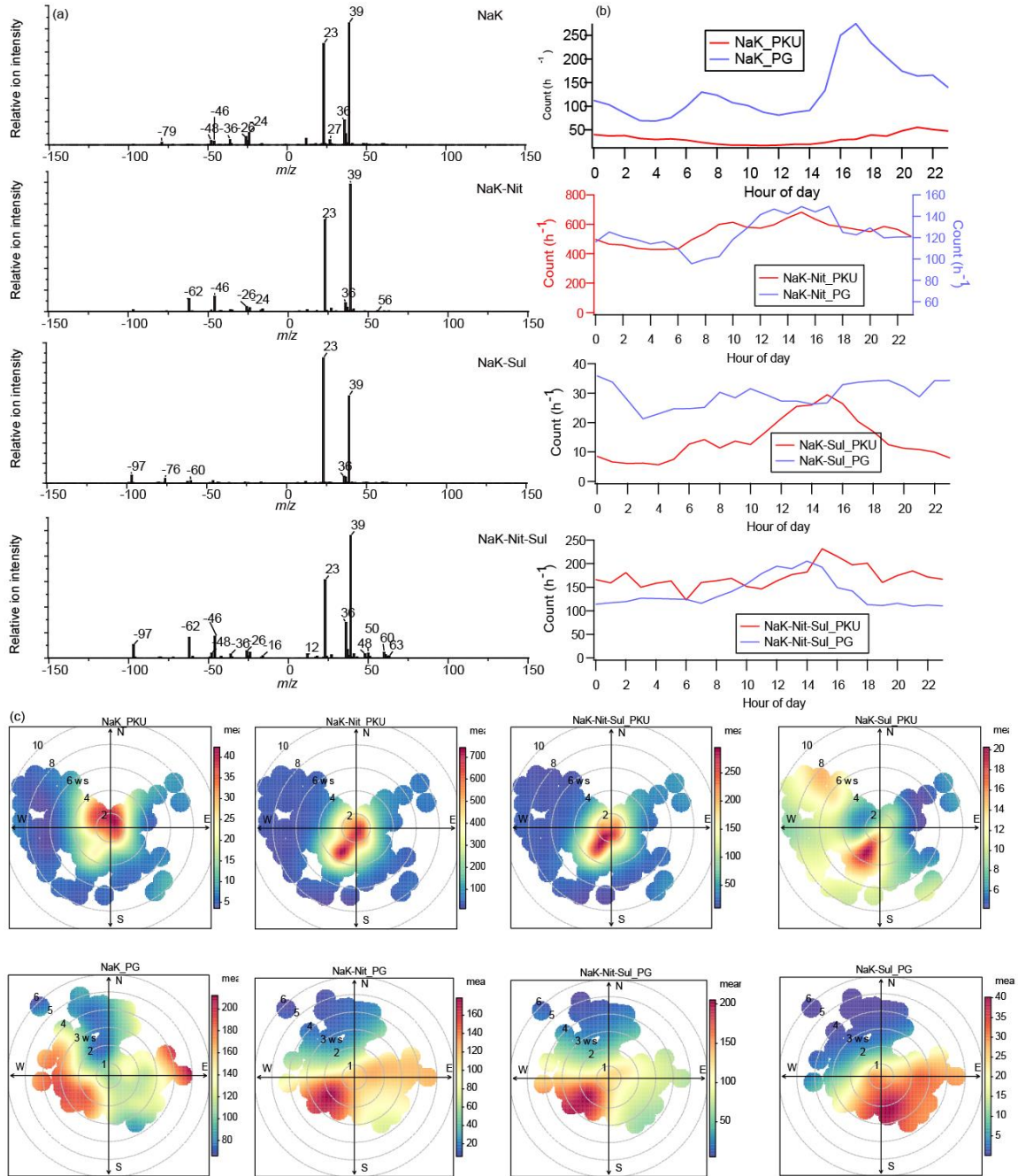
Figure 8. (a): average mass spectra of NaK, NaK-Nit, NaK-Nit-Sul, and NaK-Sul observed

at both sites; (b): diurnal patterns of the hourly count of NaK, NaK-Nit, NaK-Nit-Sul, and

NaK-Sul at both sites; (c): polar plots of NaK, NaK-Nit, NaK-Nit-Sul, and NaK-Sul; the

grey circles indicate wind speed (m s^{-1}).

3.3 Unique Particle types at the PKU site

OC-Nit_PKU (0.9%) and ECOC-Nit_PKU (3.1%) with strong ion intensities of nitrate were observed at the PKU site. OC-Nit_PKU and ECOC-Nit_PKU showed a peak at night than at daytime, similar to the diurnal profiles of OC-Nit-Sul_PKU and ECOC-Nit-Sul_PKU. Such nitrate-rich particle types could have come from the uptake of nitrate in OC and ECOC(Qin et al., 2012; Chen et al., 2016). Polar plots suggest that both types were formed locally when the wind speed was lower than 4 ms^{-1}. The NO_x-rich environment in urban Beijing provides a favorable condition for nitrate formation at night (Wang et al., 2016; Shi et al., 2019).

A minor amount (0.10%) of amine-containing particles was observed at the PKU site, and trimethylamine ion fragments (m/z 58 and 59) were influential in the mass spectrum of K-amine-Nit-Sul_PKU (Figure 9a). The diurnal profile of K-amine-Nit-Sul_PKU showed an afternoon peak, indicating a regional source (Figure 9c). K-amine-Nit-Sul_PKU was transported to the site from nearby locations. The amines may come from animal husbandry, BB, traffic, or vegetation (Chen et al., 2019b). Amines were ubiquitous in the atmospheric environment, playing essential roles in new particle formation and growth, as well as fog and cloud processing (Ge et al., 2011; Chen et al., 2019b).

366
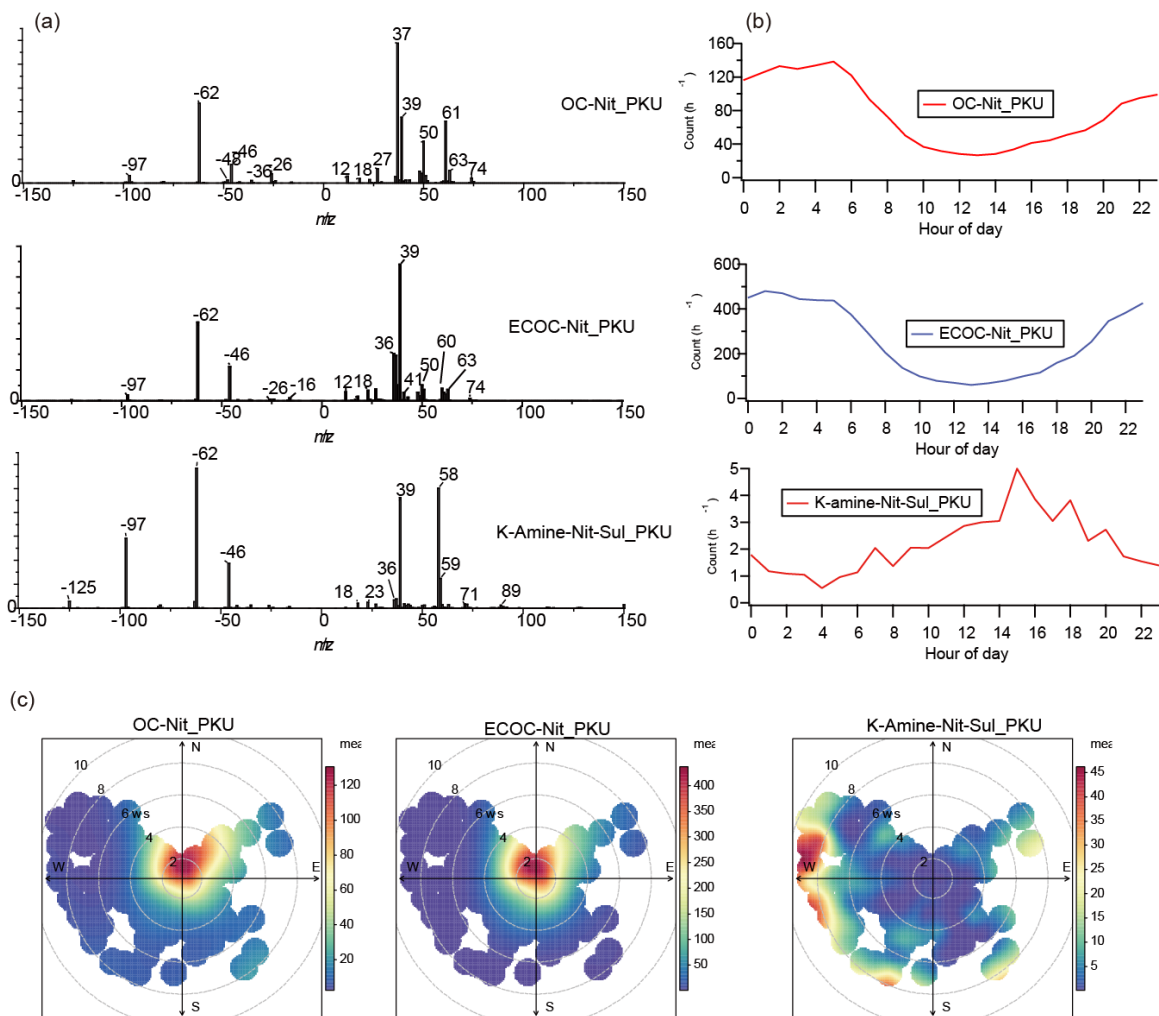
Figure 9. (a): average mass spectra of OC-Nit_PKU, ECOC-Nit_PKU, and K-amine-Nit-Sul_PKU observed at the PKU site; (b): diurnal patterns of the hourly count of OC-Nit_PKU, ECOC-Nit_PKU, and K-amine-Nit-Sul_PKU at the PKU site; (c): polar plots of OC-Nit_PKU, ECOC-Nit_PKU, and K-amine-Nit-Sul_PKU, and the grey circles indicate wind speed (m s^{-1}).

3.4 Unique Particle types at the PG site

OC_PG (5.9%) and ECOC_PG (3.3%) were only observed at the rural site PG (Figure 10). The major components of these two types were consistent with the OC and ECOC

25

375 categories, respectively, but with limited uptake of sulfate and nitrate, suggesting that they

376 were possibly freshly emitted particles(Peng et al., 2020b). Their diurnal profiles are

377 consistent with cooking and heating patterns which peaked at 07:00 in the morning and

378 17:00. Polar plots suggest that OC_PG mainly came from nearby and other remote areas

379 in all directions except the north. ECOC mainly came from the east of the PG site. These

380 results supported the assumption that the two types were mainly from local emission

381 sources. Also, the emission of OC_PG and ECOC_PG is popular in the region.
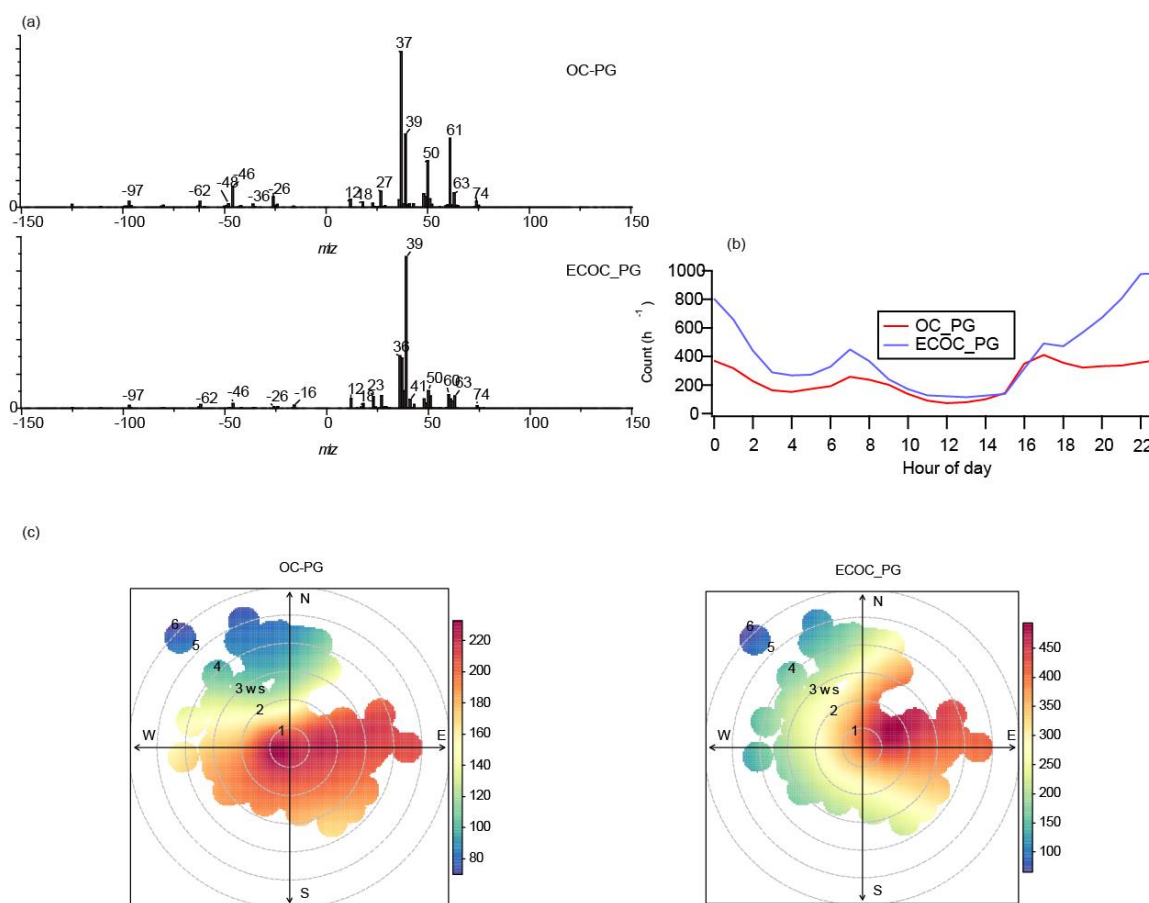
382

383 Figure 10. (a) Average mass spectra of OC_PG and ECOC_PG, (c) diurnal plots of OC_PG

384 and ECOC_PG, and (c) polar plots of OC_PG and ECOC_PG. All these particle types

385 appeared at the PG site.

4. Discussion

Multiple source apportionment models have been used in Beijing to quantify the sources of particles (Sun et al., 2014a; Xu et al., 2015; Zhai et al., 2016). Biomass burning, coal combustion, traffic, and dust are the key sources of PM (Sun et al., 2014a; Liu et al., 2018; Huang et al., 2014). Multiple studies confirmed that biomass burning is an essential source of PM in urban Beijing (Gao et al., 2014; Huang et al., 2014; Sun et al., 2014a; Zheng et al., 2017). In this study, biomass burning, and other solid fuel burning were identified as crucial sources of PM in not only urban but also rural areas of Beijing. We observed that BB-related particles (K-rich category) were more abundant at PG than at PKU. In particular, we found fresh-emitted K-containing particles at the Pinggu site, confirmed the importance of local emissions to PM. Furthermore, K-containing particles in the urban area were more aged, suggested that they are aged and mostly from the surrounding areas. The result is consistent with the results from (Liu et al., 2019b) based on a combined receptor and footprint models. Nevertheless, household emissions in the BHT region caused 32% and 15% of primary $PM_{2.5}$ and SO_2. These studies have proved the importance of household emission from BB in the BHT area (Liu et al., 2016a). Especially at the PG site, the ambient PM was mainly controlled by long-range transport and household emissions from cooking and heating.

Due to the nature of SPAMS, the chemical composition of PM cannot be precisely quantified. However, single particle aerosol mass spectrometers have advantages in studying the chemical composition, mixing state, source, and process of particles (Pratt and Prather, 2012). Mass-based technologies can not differentiate the origin of the bulk of nitrate, whether it is transported or formed locally. Indeed, single particle types in urban

409 Beijing have been reported in previous studies (Li et al., 2014; Liu et al., 2016b), and the

410 major types are consistent with this study. However, in this study, we adopted a cluster

411 strategy considering the relative ion peak area of sulfate and nitrate as indicators of particle

412 processing. Therefore, more details could be extracted from both two simultaneous datasets.

413 We confirmed that the source, origination, and processes were different for these particles

414 in the urban and rural areas. For example, the seriously processed particles, such as K-Nit-

415 Sul, OC-Nit-Sul, and NaK-Nit-Sul, acted with no distinct diurnal patterns as background

416 or regional sources (Xie et al., 2019). The processed particles, such as OC-Nit, ECOC-Nit,

417 and NaK-Nit, were affected by emissions and secondary formations.

418 The emission and transport patterns were different in the urban and rural areas, resulting in

419 different characteristics of PM. For example, EC particles were a key component at PKU

420 (18.2% in total), but a minor particle type at PG (5.6%). Meanwhile, in the urban area of

421 Beijing, direct emission of K-rich particles should be limited due to strict control measures;

422 thus, the K-Nit-Sul particles are mainly from long-range transport. Transported particles

423 were aged and commonly coated a thick layer of nitrate and sulfate, but the local particles

424 were affected by both emission and the near-surface aging process. For example, at PKU,

425 the primary emission sources were traffic and central heating supply, causing a NO_x-rich

426 region in which freshly-emitted particle types could undergo processing due to the uptake

427 of nitrate (Wang et al., 2016). In the nearby villages of PG, domestic heating and cooking

428 were the major contributors of primary particles when the temperature was low in the

429 morning and afternoon, resulting in the emission of multiple primary particle types such as

430 OC_PG and ECOC_PG. In short, the characteristics of PM in urban and rural areas of

431 Beijing were affected by local emissions and interacted with each other due to regional

432 transport.

433 SO$_2$ was strictly controlled in Beijing. However, the emission of SO$_2$ is still significant in

434 the nearby Hebei and Shandong provinces (Shi et al. 2019). The different control measures

435 produced a low concentration area of SO$_2$ around Beijing. Sulfate-rich particle types such

436 as EC-Sul, OC-Sul, K-Sul, and NaK-Sul usually arrived at the PKU site when the wind

437 speed was high (> 3m s^{-1}). The wind directions, along with the transport of sulfate-rich

438 particles, were east, southwest and south. In these directions, sulfate was either primarily

439 emitted from coal burning for residential heating, power generation and industry, or

440 secondary uptake on pre-existing particles (Zhang et al., 2015; Peng et al., 2020a).

441 Likewise, a portion of sulfate-rich particle arrived at the PG site when the wind speed was

442 high. However, locally formed sulfate was also pronounced, especially for ECOC-Sul, K-

443 Sul, and NaK-Sul. As discussed in Section 3, ECOC-Sul and NaK-Sul were mainly from

444 coal burning for residential heating, and K-Sul was formed due to the uptake of secondary

445 sulfate. Conclusively, the particulate characterization in rural areas around Beijing is

446 significantly influenced by residential coal burning.

447 Secondary nitrate formation is still a critical issue in Beijing. The daytime arising of nitrate

448 has been reported in studies (Sun et al., 2013), and we also found a similar predominant of

449 nitrogen-containing particles in this study. Recent studies have reported the early morning

450 peaks of nitrate using a soot particle aerosol mass spectrometer (SP-AMS) (Wang et al.,

451 2019), which is consistent with our results. Interestingly, the early morning peak was only

452 observed for several particle types at both sites, including EC-Nit_PKU, K-Nit_PKU, EC-

453 Nit-Sul-PG, and EC-Nit_PG. This result is not surprising because PG is also a NO$_2$-rich

454   region (Shi et al., 2019). The increasing contribution of nitrate-containing particles

455   suggests the role of night chemistry in nitrate uptake on particles. Wang et al. (2017)

456   revealed the importance of night N_2O_5 chemistry on nocturnal nitrate formation in the

457   urban area of Beijing. The heterogeneous hydrolysis of N_2O_5 was most favorable when NO

458   was at a low level. Moreover, the polar plots suggested a small role of long-range transport

459   to the nitrate in individual particles. The contribution of local traffic was insignificant at

460   the PG site as it was far from highways and major roads, the nighttime formation of nitrate

461   appeared to be important in PG as well.

462   **5. Conclusion**

463   Two SPAMSs were simultaneously deployed at urban and rural sites in Beijing in order to

464   characterize PM during wintertime. The results at both sites indicate that they shared 17

465   types of common clusters, most of which belonged to particle categories such as EC, OC,

466   ECOC, BB, and NaK. The origins and sources of these particle types at both sampling sites

467   are also comprehensively analyzed. Most of the processed PM, including EC-Nit-Sul_PKU,

468   ECOC-Nit-Sul_PKU, and NaK-Nit-Sul_PKU, were aged locally in a NO_x-rich

469   environment, while EC-Nit-Sul_PG, ECOC-Nit-Sul_PG, NaK-Nit-Sul_PG, and OC-Nit-

470   Sul_PG were regional. Domestic heating in the rural area was found to be an important

471   source of PM, and such heating activities typically caused three diurnal peaks in the early

472   morning, morning, and afternoon (after sunset). Moreover, the early morning peak of

473   nitrate was observed at both sites, suggesting the contribution of the heterogeneous

474   hydrolysis of N_2O_5 in the dark during the winter. The insights gained in this study can

475   provide useful references for understanding the relationship between regional transport and

476   local aging in both urban and rural areas in Beijing. In Part II, we focus on haze events

477   observed at both sites and attempt to determine the effects of heating activities and possible

478   regional transport between PKU and PG.

479   *Data availability.* All data described in this study are available upon request from the

480   corresponding authors.

481   *Author contributions.* FY, MZ, TZ, QZ, and KH designed the experiments; YC, JC, ZW,

482   MT, CP, and HY carried them out; XYang, XYao, YL, GS, and ZS analyzed the

483   experimental data; YC prepared the manuscript with contributions from all coauthors.

484   *Competing interests.* The authors declare that they have no conflict of interest.

489   **References**

490   Bi, X., Zhang, G., Li, L., Wang, X., Li, M., Sheng, G., Fu, J., and Zhou, Z.: Mixing state

491   of biomass burning particles by single particle aerosol mass spectrometer in the urban area

492   of PRD, China, Atmos. Environ., 45, 3447-3453, 10.1016/j.atmosenv.2011.03.034, 2011.

493   Cai, J., Wang, J., Zhang, Y., Tian, H., Zhu, C., Gross, D. S., Hu, M., Hao, J., He, K., and

494   Wang, S.: Source apportionment of Pb-containing particles in Beijing during January 2013,

495   Environ Pollut, 226, 30-40, 2017.

496   Chen, Y., Cao, J., Huang, R., Yang, F., Wang, Q., and Wang, Y.: Characterization, mixing

497   state, and evolution of urban single particles in Xi'an (China) during wintertime haze days,

498   Sci. Total Environ., 573, 937-945, 10.1016/j.scitotenv.2016.08.151, 2016.

499   Chen, Y., Wenger, J. C., Yang, F., Cao, J., Huang, R., Shi, G., Zhang, S., Tian, M., and

500   Wang, H.: Source characterization of urban particles from meat smoking activities in

501   Chongqing, China using single particle aerosol mass spectrometry, Environ. Pollut., 228,

502   92-101, 10.1016/j.envpol.2017.05.022, 2017.

503   Chen, Y., Liu, H., Huang, R. J., Yang, F., Tian, M., Yao, X., Shen, Z., Yan, L., and Cao,

504   J.: Atmospheric Processing of Loess Particles in a Polluted Urban Area of Northwestern

505   China, J. Geophys. Res. Atmos., 124, 7919-7929, 10.1029/2018jd029956, 2019a.

506   Chen, Y., Tian, M., Huang, R.-J., Shi, G., Wang, H., Peng, C., Cao, J., Wang, Q., Zhang,

507   S., Guo, D., Zhang, L., and Yang, F.: Characterization of urban amine-containing particles

508   in southwestern China: seasonal variation, source, and processing, Atmos. Chem. Phys.,

509   19, 3245-3255, 10.5194/acp-19-3245-2019, 2019b.

510   Cheng, Y., Zheng, G., Wei, C., Mu, Q., Zheng, B., Wang, Z., Gao, M., Zhang, Q., He, K.,

511   and Carmichael, G.: Reactive nitrogen chemistry in aerosol water as a source of sulfate

512   during haze events in China, Science Advances, 2, e1601530, 2016.

513   Dall'osto, M., and Harrison, R.: Chemical characterisation of single airborne particles in

514   Athens   (Greece)   by   ATOFMS,   Atmos.   Environ.,   40,   7614-7631,

515   10.1016/j.atmosenv.2006.06.053, 2006.

516   Dall'Osto, M., Beddows, D., McGillicuddy, E. J., Esser-Gietl, J. K., Harrison, R. M., and

517   Wenger, J. C.: On the simultaneous deployment of two single-particle mass spectrometers

at an urban background and a roadside site during SAPUSS, Atmos. Chem. Phys., 16, 9693-9710, 2016.

Day, D. A., Liu, S., Russell, L. M., and Ziemann, P. J.: Organonitrate group concentrations in submicron particles with high nitrate and organic fractions in coastal southern California, Atmos Environ, 44, 1970-1979, 10.1016/j.atmosenv.2010.02.045, 2010.

Du, W., Zhao, J., Wang, Y., Zhang, Y., Wang, Q., Xu, W., Chen, C., Han, T., Zhang, F., Li, Z., Fu, P., Li, J., Wang, Z., and Sun, Y.: Simultaneous measurements of particle number size distributions at ground level and 260 m on a meteorological tower in urban Beijing, China, Atmos. Chem. Phys., 17, 6797-6811, 10.5194/acp-17-6797-2017, 2017.

Gao, J., Zhang, Y., Zhang, M., Zhang, J., Wang, S., Tao, J., Wang, H., Luo, D., Chai, F., and Ren, C.: Photochemical properties and source of pollutants during continuous pollution episodes in Beijing, October, 2011, J Environ Sci-China, 26, 44-53, 10.1016/s1001-0742(13)60379-4, 2014.

Gard, E., Mayer, J. E., Morrical, B. D., Dienes, T., Fergenson, D. P., and Prather, K. A.: Real-time analysis of individual atmospheric aerosol particles: Design and performance of a portable ATOFMS, Anal. Chem., 69, 4083-4091, 1997.

Ge, X., Wexler, A. S., and Clegg, S. L.: Atmospheric amines – Part I. A review, Atmos. Environ., 45, 524-546, 10.1016/j.atmosenv.2010.10.012, 2011.

Guo, S., Hu, M., Guo, Q., Zhang, X., Zheng, M., Zheng, J., Chang, C. C., Schauer, J. J., and Zhang, R.: Primary sources and secondary formation of organic aerosols in Beijing, China, Environ. Sci. Technol., 46, 9846-9853, 10.1021/es2042564, 2012.

33

539 Guo, S., Hu, M., Zamora, M. L., Peng, J., Shang, D., Zheng, J., Du, Z., Wu, Z., Shao, M.,

540 Zeng, L., Molina, M. J., and Zhang, R.: Elucidating severe urban haze formation in China,

541 Proc. Natl. Acad. Sci. U.S.A., 111, 17373-17378, 10.1073/pnas.1419604111, 2014.

542 He, K., Yang, F., Ma, Y., Zhang, Q., Yao, X., Chan, C. K., Cadle, S., Chan, T., and Mulawa,

543 P.: The characteristics of PM2.5 in Beijing, China, Atmos. Environ., 35, 4959-4970,

544 10.1016/s1352-2310(01)00301-6, 2001.

545 Healy, R. M., Hellebust, S., Kourtchev, I., Allanic, A., amp, apos, Connor, I. P., Bell, J.

546 M., Healy, D. A., Sodeau, J. R., and Wenger, J. C.: Source apportionment of PM2.5 in

547 Cork Harbour, Ireland using a combination of single particle mass spectrometry and

548 quantitative semi-continuous measurements, Atmos. Chem. Phys., 10, 9593-9613,

549 10.5194/acp-10-9593-2010, 2010.

550 Healy, R. M., Sciare, J., Poulain, L., Kamili, K., Merkel, M., Müller, T., Wiedensohler, A.,

551 Eckhardt, S., Stohl, A., Sarda-Estève, R., McGillicuddy, E., amp, apos, Connor, I. P.,

552 Sodeau, J. R., and Wenger, J. C.: Sources and mixing state of size-resolved elemental

553 carbon particles in a European megacity: Paris, Atmos. Chem. Phys., 12, 1681-1700,

554 10.5194/acp-12-1681-2012, 2012.

555 Huang, M., Hao, L., Guo, X., Hu, C., Gu, X., Zhao, W., Wang, Z., Fang, L., and Zhang,

556 W.: Characterization of secondary organic aerosol particles using aerosol laser time-of-

557 flight mass spectrometer coupled with FCM clustering algorithm, Atmos. Environ., 64, 85-

558 94, 10.1016/j.atmosenv.2012.09.044, 2013.

559 Huang, R. J., Zhang, Y., Bozzetti, C., Ho, K. F., Cao, J. J., Han, Y., Daellenbach, K. R.,

560 Slowik, J. G., Platt, S. M., Canonaco, F., Zotter, P., Wolf, R., Pieber, S. M., Bruns, E. A.,

561   Crippa, M., Ciarelli, G., Piazzalunga, A., Schwikowski, M., Abbaszade, G., Schnelle-Kreis,

562   J., Zimmermann, R., An, Z., Szidat, S., Baltensperger, U., El Haddad, I., and Prevot, A. S.:

563   High secondary aerosol contribution to particulate pollution during haze events in China,

564   Nature, 514, 218-222, 10.1038/nature13774, 2014.

565   Huang, X.-F., He, L.-Y., Hu, M., and Zhang, Y.-H.: Annual variation of particulate organic

566   compounds in PM2.5 in the urban atmosphere of Beijing, Atmos. Environ., 40, 2449-2458,

567   10.1016/j.atmosenv.2005.12.039, 2006.

568   Huang, X. F., He, L. Y., Hu, M., Canagaratna, M. R., Sun, Y., Zhang, Q., Zhu, T., Xue, L.,

569   Zeng, L. W., Liu, X. G., Zhang, Y. H., Jayne, J. T., Ng, N. L., and Worsnop, D. R.: Highly

570   time-resolved chemical characterization of atmospheric submicron particles during 2008

571   Beijing Olympic Games using an Aerodyne High-Resolution Aerosol Mass Spectrometer,

572   Atmos. Chem. Phys., 10, 8933-8945, 10.5194/acp-10-8933-2010, 2010.

573   Li, L., Huang, Z., Dong, J., Li, M., Gao, W., Nian, H., Fu, Z., Zhang, G., Bi, X., Cheng, P.,

574   and Zhou, Z.: Real time bipolar time-of-flight mass spectrometer for analyzing single

575   aerosol particles, Int. J. Mass spectrom., 303, 118-124, 10.1016/j.ijms.2011.01.017, 2011.

576   Li, L., Li, M., Huang, Z., Gao, W., Nian, H., Fu, Z., Gao, J., Chai, F., and Zhou, Z.:

577   Ambient particle characterization by single particle aerosol mass spectrometry in an urban

578   area of Beijing, Atmos. Environ., 94, 323-331, 10.1016/j.atmosenv.2014.03.048, 2014.

579   Li, P., Yan, R., Yu, S., Wang, S., Liu, W., and Bao, H.: Reinstate regional transport of

580   PM2.5 as a major cause of severe haze in Beijing, Proc Natl Acad Sci U S A, 112, E2739-

581   2740, 10.1073/pnas.1502596112, 2015.

582 Liu, D., Joshi, R., Wang, J., Yu, C., Allan, J. D., Coe, H., Flynn, M. J., Xie, C., Lee, J.,

583 Squires, F., Kotthaus, S., Grimmond, S., Ge, X., Sun, Y., and Fu, P.: Contrasting physical

584 properties of black carbon in urban Beijing between winter and summer, Atmos. Chem.

585 Phys., 19, 6749-6769, 10.5194/acp-19-6749-2019, 2019a.

586 Liu, J., Mauzerall, D. L., Chen, Q., Zhang, Q., Song, Y., Peng, W., Klimont, Z., Qiu, X.,

587 Zhang, S., Hu, M., Lin, W., Smith, K. R., and Zhu, T.: Air pollutant emissions from

588 Chinese households: A major and underappreciated ambient pollution source, Proceedings

589 of the National Academy of Sciences, 113, 7756-7761, 10.1073/pnas.1604537113, 2016a.

590 Liu, L., Wang, Y., Du, S., Zhang, W., Hou, L., Vedal, S., Han, B., Yang, W., Chen, M.,

591 and Bai, Z.: Characteristics of atmospheric single particles during haze periods in a typical

592 urban area of Beijing: A case study in October, 2014, J Environ Sci-China, 40, 145-153,

593 10.1016/j.jes.2015.10.027, 2016b.

594 Liu, Y., Zheng, M., Yu, M., Cai, X., Du, H., Li, J., Zhou, T., Yan, C., Wang, X., Shi, Z.,

595 Harrison, R. M., Zhang, Q., and He, K.: High Time Resolution Source Apportionment of

596 PM$_{2.5}$ in Beijing with Multiple Models, Atmospheric Chemistry

597 and Physics Discussions, 2018, 1-31, 10.5194/acp-2018-1234, 2018.

598 Liu, Y., Zheng, M., Yu, M., Cai, X., Du, H., Li, J., Zhou, T., Yan, C., Wang, X., Shi, Z.,

599 Harrison, R. M., Zhang, Q., and He, K.: High-time-resolution source apportionment of

600 PM$_{2.5}$ in Beijing with multiple models, Atmos Chem Phys, 19,

601 6595-6609, 10.5194/acp-19-6595-2019, 2019b.

602 Ma, L., Li, M., Huang, Z., Li, L., Gao, W., Nian, H., Zou, L., Fu, Z., Gao, J., Chai, F., and

603 Zhou, Z.: Real time analysis of lead-containing atmospheric particles in Beijing during

36

604   springtime by single particle aerosol mass spectrometry, Chemosphere, 154, 454-462,

605   10.1016/j.chemosphere.2016.04.001, 2016.

606   McGuire, M. L., Jeong, C. H., Slowik, J. G., Chang, R. Y. W., Corbin, J. C., Lu, G., Mihele,

607   C., Rehbein, P. J. G., Sills, D. M. L., Abbatt, J. P. D., Brook, J. R., and Evans, G. J.:

608   Elucidating determinants of aerosol composition through particle-type-based receptor

609   modeling, Atmos. Chem. Phys., 11, 8133-8155, 10.5194/acp-11-8133-2011, 2011.

610   Pagels, J., Dutcher, D. D., Stolzenburg, M. R., McMurry, P. H., Gälli, M. E., and Gross, D.

611   S.: Fine-particle emissions from solid biofuel combustion studied with single-particle mass

612   spectrometry: Identification of markers for organics, soot, and ash components, J. Geophys.

613   Res. Atmos., 118, 859-870, 10.1029/2012jd018389, 2013.

614   Peng, C., Tian, M., Wang, X., Yang, F., Shi, G., Huang, R.-J., Yao, X., Wang, Q., Zhai,

615   C., Zhang, S., Qian, R., Cao, J., and Chen, Y.: Light absorption of brown carbon in PM2.5

616   in the Three Gorges Reservoir region, southwestern China: Implications of biomass

617   burning and secondary formation, Atmos. Environ., 229, 117409,

618   10.1016/j.atmosenv.2020.117409, 2020a.

619   Peng, C., Yang, F., Tian, M., Shi, G., Li, L., Huang, R. J., Yao, X., Luo, B., Zhai, C., and

620   Chen, Y.: Brown carbon aerosol in two megacities in the Sichuan Basin of southwestern

621   China: Light absorption properties and implications, Sci. Total Environ., 719, 137483,

622   10.1016/j.scitotenv.2020.137483, 2020b.

623   Pratt, K. A., and Prather, K. A.: Mass spectrometry of atmospheric aerosols--recent

624   developments and applications. Part II: On-line mass spectrometry techniques, Mass

625   Spectrom. Rev., 31, 17-48, 10.1002/mas.20330, 2012.

626 Qin, X., Pratt, K. A., Shields, L. G., Toner, S. M., and Prather, K. A.: Seasonal comparisons

627 of single-particle chemical mixing state in Riverside, CA, Atmos. Environ., 59, 587-596,

628 10.1016/j.atmosenv.2012.05.032, 2012.

629 Shi, Z., Vu, T., Kotthaus, S., Harrison, R. M., Grimmond, S., Yue, S., Zhu, T., Lee, J., Han,

630 Y., Demuzere, M., Dunmore, R. E., Ren, L., Liu, D., Wang, Y., Wild, O., Allan, J., Acton,

631 W. J., Barlow, J., Barratt, B., Beddows, D., Bloss, W. J., Calzolai, G., Carruthers, D.,

632 Carslaw, D. C., Chan, Q., Chatzidiakou, L., Chen, Y., Crilley, L., Coe, H., Dai, T., Doherty,

633 R., Duan, F., Fu, P., Ge, B., Ge, M., Guan, D., Hamilton, J. F., He, K., Heal, M., Heard,

634 D., Hewitt, C. N., Hollaway, M., Hu, M., Ji, D., Jiang, X., Jones, R., Kalberer, M., Kelly,

635 F. J., Kramer, L., Langford, B., Lin, C., Lewis, A. C., Li, J., Li, W., Liu, H., Liu, J., Loh,

636 M., Lu, K., Lucarelli, F., Mann, G., McFiggans, G., Miller, M. R., Mills, G., Monk, P.,

637 Nemitz, E., O'Connor, F., Ouyang, B., Palmer, P. I., Percival, C., Popoola, O., Reeves, C.,

638 Rickard, A. R., Shao, L., Shi, G., Spracklen, D., Stevenson, D., Sun, Y., Sun, Z., Tao, S.,

639 Tong, S., Wang, Q., Wang, W., Wang, X., Wang, X., Wang, Z., Wei, L., Whalley, L., Wu,

640 X., Wu, Z., Xie, P., Yang, F., Zhang, Q., Zhang, Y., Zhang, Y., and Zheng, M.: Introduction

641 to the special issue "In-depth study of air pollution sources and processes within Beijing

642 and its surrounding region (APHH-Beijing)", Atmos. Chem. Phys., 19, 7519-7546,

643 10.5194/acp-19-7519-2019, 2019.

644 Silva, P. J., Liu, D.-Y., Noble, C. A., and Prather, K. A.: Size and Chemical

645 Characterization of Individual Particles Resulting from Biomass Burning of Local

646 Southern California Species, Environ. Sci. Technol., 33, 3068-3076, 10.1021/es980544p,

647 1999.

648   Silva, P. J., Carlin, R. A., and Prather, K. A.: Single particle analysis of suspended soil dust

649   from Southern California, Atmos Environ, 34, 1811-1820, 10.1016/S1352-

650   2310(99)00338-6, 2000.

651   Sodeman, D. A., Toner, S. M., and Prather, K. A.: Determination of single particle mass

652   spectral signatures from light-duty vehicle emissions, Environ. Sci. Technol., 39, 4569-

653   4580, 10.1021/es0489947, 2005.

654   Sullivan, R. C., Guazzotti, S. A., Sodeman, D. A., Tang, Y., Carmichael, G. R., and Prather,

655   K. A.: Mineral dust is a sink for chlorine in the marine boundary layer, Atmos. Environ.,

656   41, 7166-7179, 10.1016/j.atmosenv.2007.05.047, 2007.

657   Sun, Y., Jiang, Q., Wang, Z., Fu, P., Li, J., Yang, T., and Yin, Y.: Investigation of the

658   sources and evolution processes of severe haze pollution in Beijing in January 2013, J

659   Geophys Res, 119, 4380-4398, 2014a.

660   Sun, Y., Jiang, Q., Wang, Z., Fu, P., Li, J., Yang, T., and Yin, Y.: Investigation of the

661   sources and evolution processes of severe haze pollution in Beijing in January 2013, J.

662   Geophys. Res. Atmos., 119, 4380-4398, 10.1002/2014jd021641, 2014b.

663   Sun, Y. L., Wang, Z. F., Fu, P. Q., Yang, T., Jiang, Q., Dong, H. B., Li, J., and Jia, J. J.:

664   Aerosol composition, sources and processes during wintertime in Beijing, China, Atmos.

665   Chem. Phys., 13, 4577-4592, 10.5194/acp-13-4577-2013, 2013.

666   Tao, S., Wang, X., Chen, H., Yang, X., Li, M., Li, L., and Zhou, Z.: Single particle analysis

667   of ambient aerosols in Shanghai during the World Exposition, 2010: two case studies, Front

668   Environ Sci En, 5, 391-401, 10.1007/s11783-011-0355-x, 2011.

669   Toner, S. M., Shields, L. G., Sodeman, D. A., and Prather, K. A.: Using mass spectral

670   source signatures to apportion exhaust particles from gasoline and diesel powered vehicles

671   in a freeway study using UF-ATOFMS, Atmos. Environ., 42, 568-581,

672   10.1016/j.atmosenv.2007.08.005, 2008.

673   Wang, G., Zhang, R., Gomez, M. E., Yang, L., Levy Zamora, M., Hu, M., Lin, Y., Peng,

674   J., Guo, S., Meng, J., Li, J., Cheng, C., Hu, T., Ren, Y., Wang, Y., Gao, J., Cao, J., An, Z.,

675   Zhou, W., Li, G., Wang, J., Tian, P., Marrero-Ortiz, W., Secrest, J., Du, Z., Zheng, J.,

676   Shang, D., Zeng, L., Shao, M., Wang, W., Huang, Y., Wang, Y., Zhu, Y., Li, Y., Hu, J.,

677   Pan, B., Cai, L., Cheng, Y., Ji, Y., Zhang, F., Rosenfeld, D., Liss, P. S., Duce, R. A., Kolb,

678   C. E., and Molina, M. J.: Persistent sulfate formation from London Fog to Chinese haze,

679   Proc. Natl. Acad. Sci. U.S.A., 113, 13630-13635, 10.1073/pnas.1616540113, 2016.

680   Wang, H., Zhu, B., Zhang, Z., An, J., and Shen, L.: Mixing state of individual carbonaceous

681   particles during a severe haze episode in January 2013, Nanjing, China, Particuology, 20,

682   16-23, 10.1016/j.partic.2014.06.013, 2015.

683   Wang, H., Lu, K., Chen, X., Zhu, Q., Chen, Q., Guo, S., Jiang, M., Li, X., Shang, D., Tan,

684   Z., Wu, Y., Wu, Z., Zou, Q., Zheng, Y., Zeng, L., Zhu, T., Hu, M., and Zhang, Y.: High

685   N2O5 Concentrations Observed in Urban Beijing: Implications of a Large Nitrate

686   Formation Pathway, Environ. Sci. Technol. Lett., 4, 416-420, 10.1021/acs.estlett.7b00341,

687   2017.

688   Wang, J., Liu, D., Ge, X., Wu, Y., Shen, F., Chen, M., Zhao, J., Xie, C., Wang, Q., Xu, W.,

689   Zhang, J., Hu, J., Allan, J., Joshi, R., Fu, P., Coe, H., and Sun, Y.: Characterization of black

690   carbon-containing fine particles in Beijing during wintertime, Atmos. Chem. Phys., 19,

691   447-458, 10.5194/acp-19-447-2019, 2019.

692   Wang, P., Pan, B., Li, H., Huang, Y., Dong, X., Ai, F., Liu, L., Wu, M., and Xing, B.: The

693   Overlooked Occurrence of Environmentally Persistent Free Radicals in an Area with Low-

694   Rank Coal Burning, Xuanwei, China, Environ. Sci. Technol., 52, 1054-1061,

695   10.1021/acs.est.7b05453, 2018.

696   Xie, C., Xu, W., Wang, J., Wang, Q., Liu, D., Tang, G., Chen, P., Du, W., Zhao, J., Zhang,

697   Y., Zhou, W., Han, T., Bian, Q., Li, J., Fu, P., Wang, Z., Ge, X., Allan, J., Coe, H., and

698   Sun, Y.: Vertical characterization of aerosol optical properties and brown carbon in winter

699   in urban Beijing, China, Atmos. Chem. Phys., 19, 165-179, 10.5194/acp-19-165-2019,

700   2019.

701   Xu, J., Li, M., Shi, G., Wang, H., Ma, X., Wu, J., Shi, X., and Feng, Y.: Mass spectra

702   features of biomass burning boiler and coal burning boiler emitted particles by single

703   particle aerosol mass spectrometer, Sci Total Environ, 598, 341-352,

704   https://doi.org/10.1016/j.scitotenv.2017.04.132, 2017.

705   Xu, J., Wang, H., Li, X., Li, Y., Wen, J., Zhang, J., Shi, X., Li, M., Wang, W., Shi, G., and

706   Feng, Y.: Refined source apportionment of coal combustion sources by using single

707   particle mass spectrometry, Sci. Total Environ., 627, 633-646,

708   10.1016/j.scitotenv.2018.01.269, 2018.

709   Xu, W. Q., Sun, Y. L., Chen, C., Du, W., Han, T. T., Wang, Q. Q., Fu, P. Q., Wang, Z. F.,

710   Zhao, X. J., Zhou, L. B., Ji, D. S., Wang, P. C., and Worsnop, D. R.: Aerosol composition,

711   oxidation properties, and sources in Beijing: results from the 2014 Asia-Pacific Economic

712   Cooperation summit study, Atmos. Chem. Phys., 15, 13681-13698, 10.5194/acp-15-

713   13681-2015, 2015.

714 Zhai, J., Wang, X., Li, J., Xu, T., Chen, H., Yang, X., and Chen, J.: Thermal desorption

715 single particle mass spectrometry of ambient aerosol in Shanghai, Atmos. Environ., 123,

716 407-414, 10.1016/j.atmosenv.2015.09.001, 2015.

717 Zhai, S., An, X., Zhao, T., Sun, Z., Hou, Q., and Wang, C.: Detecting critical $PM_{2.5}$

718 emission sources and their contributions to a heavy haze episode in Beijing, China by using

719 an adjoint model, Atmospheric Chemistry and Physics Discussions, 2016, 1-20,

720 10.5194/acp-2016-911, 2016.

721 Zhang, R., Wang, G., Guo, S., Zamora, M. L., Ying, Q., Lin, Y., Wang, W., Hu, M., and

722 Wang, Y.: Formation of urban fine particulate matter, Chem. Rev., 115, 3803-3855,

723 10.1021/acs.chemrev.5b00067, 2015.

724 Zhao, J., Qiu, Y., Zhou, W., Xu, W., Wang, J., Zhang, Y., Li, L., Xie, C., Wang, Q., Du,

725 W., Worsnop, D. R., Canagaratna, M. R., Zhou, L., Ge, X., Fu, P., Li, J., Wang, Z.,

726 Donahue, N. M., and Sun, Y.: Organic Aerosol Processing During Winter Severe Haze

727 Episodes in Beijing, J. Geophys. Res. Atmos., 124, 10248-10263, 10.1029/2019jd030832,

728 2019.

729 Zheng, M., Yan, C. Q., Wang, S. X., He, K. B., and Zhang, Y. H.: Understanding PM2.5

730 sources in China: challenges and perspectives, Natl Sci Rev, 4, 801-803,

731 10.1093/nsr/nwx129, 2017.

732